The GEF Cdc24 and GAP Rga2 synergistically regulate Cdc42 GTPase cycling

Sophie Tschirpke[1], **Werner K-G. Daalman**[1], **Liedewij Laan**[1,*]

[1]Bionanoscience Department, Delft University of Technology, Delft, the Netherlands; [*]For correspondence: L.Laan@tudelft.nl

Abstract Establishing cell polarity is vital for cells, as it is required for cell division, directed growth and secretion, and motility. A well-studied model organism for polarity establishment is *Saccharomyces cerevisiae*: here the small Rho-type GTPase Cdc42 exits the cytoplasm and accumulates in one spot on the cell membrane, marking the site of bud emergence. Due to redundancy and interconnection within the regulatory network surrounding Cdc42, the molecular mechanisms driving Cdc42 accumulation continue to be a subject of intense debate. In this study, we utilize a bulk *in vitro* GTPase assay to examine the GTPase cycle of Cdc42 in combination with two of its effectors - the GDP/GTP exchange factor (GEF) Cdc24 and GTPase activating protein (GAP) Rga2. We find that Cdc24's GEF activity scales non-linearly with its concentration, which might be linked to Cdc24 di- or oligomerisation alleviating its autoinhibition. In contrast to Cdc24, Rga2 has an order of magnitude weaker GTPase cycle boosting effect which saturates at μM concentrations. Notably, Cdc24 combined with Rga2 leads to a large synergy in boosting Cdc42's GTPase activity, which we hypothesise to be caused by the elevation of the Rga2 activity through Cdc24. Our data exemplifies a novel synergy within the regulatory network of Cdc42. This synergy contributes to efficient regulation of Cdc42's GTPase cycle over a wide range of cycling rates, enabling cells to resourcefully establish polarity. As Cdc42 is highly conserved among eukaryotes, we suspect the GEF-GAP synergy to be a general regulatory property in other eukaryotes.

Introduction

Cells require robust, yet adaptable, functioning to survive in an ever-changing environment. One of such functionalities is cell polarity, which is essential for processes such as cell division, directed growth and secretion, and motility. Cell polarity refers to the morphological and functional differentiation of distinct cellular compartments in a directional manner [Vendel et al., 2019]. One aspect of polarity establishment is the non-uniform accumulation of proteins on the cell membrane, which is generally driven by biochemical feedback circuits comprising of proteins diffusing and interacting with another and with the cytoskeleton. Different organisms evolved functionally conserved yet molecularly different systems for this functionality [Glazenburg and Laan, 2023]. Examples include the Min protein system in bacteria, the polarity networks centring the GTPases Rho and Cdc42, and the PAR system in eukaryotes [Nelson, 2003, Etienne-Manneville, 2004, Wu et al., 2013, Thompson, 2013, Frey et al., 2018, Diepeveen et al., 2018].

A well-studied system for polarity establishment is that of *Saccharomyces cerevisiae*: here the cell division control protein Cdc42 exits the cytoplasm and accumulates in one spot on the cell membrane, marking the site of bud emergence (Fig. 1). Despite decades of study dedicated to Cdc42-based polarity establishment, the molecular mechanism driving Cdc42 accumulation is still heavily debated [Martin, 2015, Goryachev and Leda, 2017, Vendel et al., 2019]. The persistence of this debate can be attributed to the high level of interconnection and redundancy present in the yeast polarity system: Cdc42 is a small Rho-type GTPase with a GTP- and GDP-bound state and a post-translationally added prenyl-group which allows it to bind to membranes. Cdc42 is surrounded by a large network of regulatory proteins, that affect its GTPase activity, phosphorylation state, or membrane association. In many cases, several proteins belong to the same group of effectors,

creating redundancy within the network [Martin, 2015, Chiou et al., 2017]. Next to binding to Cdc42, most polarity proteins bind to many other polarity proteins too, and form a dynamic assembly of many loosely interacting proteins at the polarity spot [Gao et al., 2011, Daalman et al., 2020]. Additionally, several polarity proteins have the ability to oligomerise, which may enhance polarity establishment [Lang and Munro, 2022]. This complexity makes it difficult to dissect the molecular interactions of Cdc42 regulation that result in its accumulation using living cells. *In vitro* studies, where interactions can be probed in a highly controlled environment, are still comparatively scarce and focused only on a small aspect of the system and did not include interactions between different regulatory proteins.

To enhance our knowledge of the intricate mechanism of Cdc42 regulation, we set out to study Cdc42's GTPase activity, as well as its regulation by polarity proteins, *in vitro*. Cdc42 GTPase cycling is required for polarity establishment and cells in which it has been impaired fail to polarise [Wedlich-Soldner et al., 2004]. Mechanistically, Cdc42 GTPase activity involves three steps (Fig. 1): (1) binding of GTP to Cdc42, (2) hydrolysis of GTP to GDP and free phosphate, and (3) release of GDP from Cdc42. The polarity protein network contains two classes of GTPase activity regulators: GTPase activating proteins (GAPs) - such as Rga1, Rga2, Bem2, and Bem3 - boost step 2 and a GDP/GTP exchange factor (GEF) - Cdc24 - enhances step 3 [Park and Bi, 2007, Martin, 2015]. *In vitro* studies done so-far mostly focused on single reaction steps, such as the GTP hydrolysis step and the effect of GAPs [Zheng et al., 1993, Zheng et al., 1994, Zhang et al., 1997, Zhang and Zheng, 1998, Zhang et al., 1999, Zhang et al., 2001, Smith et al., 2002], the GDP/GTP exchange reaction step in conjunction with the GEF [Zheng et al., 1994, Zheng et al., 1995], or Cdc42 membrane binding and extraction by Rdi1 [Johnson et al., 2009, Johnson et al., 2012, Das et al., 2012, Golding et al., 2019]. Given the dynamic and interconnected structure of the polarity network, these studies only give a limited understanding, neglecting effects present in multi-protein systems. A recent study confirms this notion, revealing that the scaffold Bem1 enhances the GEF activity of Cdc24 [Rapali et al., 2017].

Here, we employ a bulk *in vitro* GTPase assay to study properties of the entire GTPase cycle of *S. cerevisiae* Cdc42. We examine Cdc42 alone and in combination with its effectors - the GEF Cdc24 and GAP Rga2. These proteins are interesting study targets as they regulate distinct steps of the Cdc42 GTPase cycle, and so-far their impact was only studied with assays assessing the respective sub-step. Cdc24 is an essential protein and the only GEF present at the polarity site [Daalman et al., 2020], and Rga2 has not yet been characterised as full-length protein [Smith et al., 2002]. Further, both proteins have the potential to oligomerise: Cdc24 has been shown to oligomerise *in vitro* [Mionnet et al., 2008] and Rga2 self-interacts *in vivo* [Tarassov et al., 2008, Schlecht et al., 2012]. Oligomerisation could result in a dosage-dependent effect of Cdc24 and Rga2. Lastly, Cdc24 and Rga2 have been shown to interact *in vivo* (although it is unclear whether their interaction is direct or indirect) [Chollet et al., 2020]. In combination Cdc24 and Rga2 could synergise, inhibit each other, or have no interplay. It is conceivable that a Cdc24-Rga2 interaction could have an impact, as it has been shown that Cdc24's GEF activity is increased when it is bound to Bem1 [Rapali et al., 2017].

We find that the GEF activity of Cdc24 exhibits a non-linear dependence on its concentration, which we hypothesise to be linked to Cdc24 di- or oligomerisation and a release of its autoinhibition [Shimada et al., 2004, Mionnet et al., 2008]. Rga2 has an order of magnitude weaker GTPase cycle boosting effect than Cdc24, which saturates around 0.5 µM, which could be due to self-inhibitory di- or oligomeric structures or because at this concentration GTP hydrolysis is no longer the rate-limiting step in the GTPase cycle of Cdc42. Notably, the presence of both Cdc24 and Rga2 leads to a large synergy, an order of magnitude greater than the effect of Cdc24 alone. We also find that proteins such as Bovine serum albumin (BSA) or Casein, that are not part of the yeast polarity network, enhance Cdc42's GTPase activity and show synergy with Cdc24. The enhanced GTPase activity of Cdc42 in presence of BSA/Casein could be because BSA/Casein increase the effective Cdc42 concentration in the assay or due to an unknown interaction/mechanism between Cdc42 and BSA/Casein.

Our data shows a novel synergy between a GEF and GAP. It emphasises that in order to understand protein network functions, the network components have to be studied together; components with a rather weak individual effect (such as Rga2) can have a large synergistic impact together with other components (as Cdc24). Given the high conservation of Cdc42 across eukaryotes, we propose that the regulatory interplay between GEFs and GAPs represents a general regulatory mechanism shared among other eukaryotes.

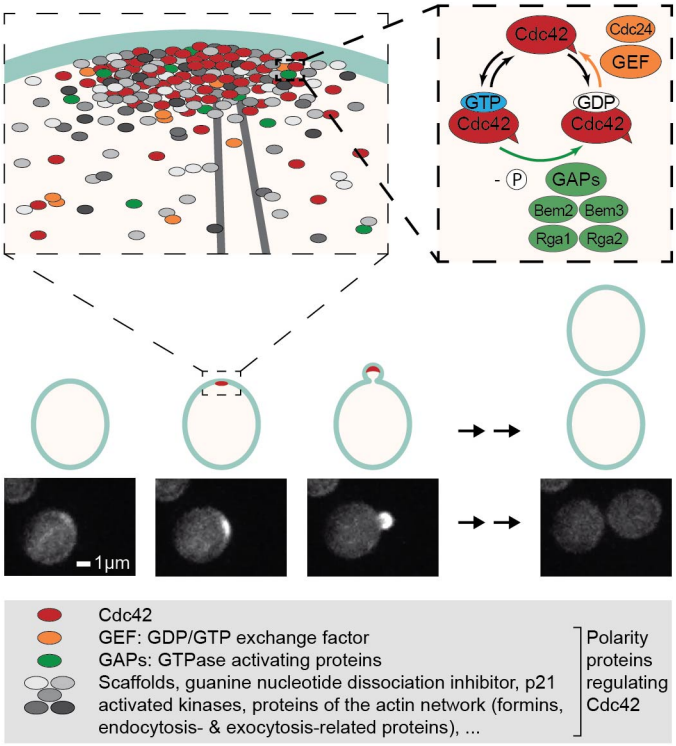

Figure 1. A complex network of polarity proteins regulates Cdc42 activity *in vivo* to establish cell polarity. The accumulation of the small Rho-GTPase Cdc42 in one spot on the cell membrane establishes cellular polarity, initiating cell division of *Saccharomyces cerevisiae*. Cdc42 is shown in red in the cartoon and in white in life cell microscopy images (bottom). Polarity establishment is driven by interactions between Cdc42 and polarity proteins of an intricate network. Of these a GEF and GAPs regulate Cdc42 GTPase cycling, a process required for its functioning in polarity establishment (top).

Abbreviations:

BSA	Bovine serum albumin
GAP	GTPase activating protein
GEF	GDP/GTP exchange factor

Results

Cdc42 GTPase activity can be reconstituted *in vitro*

So-far, properties of Cdc42's GTPase activity have been studied using the MESG/phosphorylase system [Zhang et al., 1997] or N-methylanthraniloyl-GTP/GDP [Rapali et al., 2017] system, which examine only the GTP hydrolysis or GDP release step. We here use the GTPase-Glo™ assay (Promega) to examine the entire GTPase cycle of Cdc42, allowing us to study the interplay of regulators acting on different steps of the GTPase cycle.

In each assay, Cdc42, alone or in combination with one or multiple effector proteins, is mixed with GTP and incubated at 30°C for 1-1.5 h for GTPase cycling to occur (Fig. 2). Then the reaction is stopped through transforming, in two follow-up steps, the remaining GTP to luminescent ATP. The luminescent signal of each reaction mixture is then measured. As the decrease of the GTP concentration during GTPase cycling is well fitted by an exponential model (S3, and derived in S1), which is used to obtain the rates of Cdc42 and Cdc42-effector interactions (Fig. 2).

We first analysed the GTPase activity of Cdc42 alone (Fig. 3a) through fitting the data with

$$[\mathrm{GTP}]_t = [\mathrm{GTP}]_{0h} \exp(-Kt)$$
$$\text{using } [\mathrm{GTP}]_{0h} = 1 \text{ and } K = K_1 + K_2 = k_1[\mathrm{Cdc42}] + k_2[\mathrm{Cdc42}]^2 \quad (1)$$

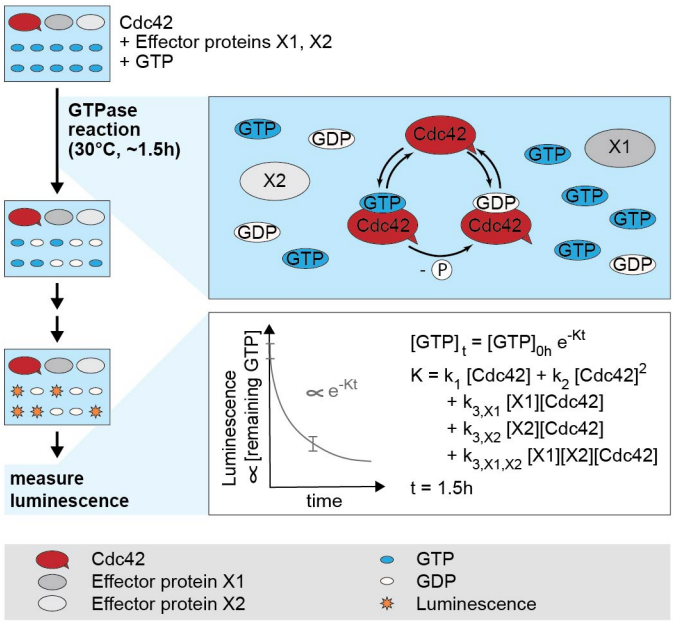

Figure 2. Reconstitution of Cdc42 GTPase regulation *in vitro*. Bulk *in vitro* GTPase assays (GTPase-Glo^{TM} assay, Promega) allow to study the GTPase cycling of Cdc42. Cdc42, alone or in combination with effector proteins, is incubated with GTP at 30°C for ~1.5 h in which GTPase cycling occurs. After two processing steps, the amount of remaining GTP, measured as luminescence, is assessed. GTP hydrolysis cycling rates can be extracted by fitting the data with an exponential model.

Here K stands for the overall GTP hydrolysis rate. We included terms that depend linearly and quadratically on the Cdc42 concentration in the model, the latter representing any possible effects due to cooperativity from dimeric Cdc42. Many GTPases have the ability to form di- and multimers, and it can still not be excluded that *S. cerevisiae* Cdc42 does (as discussed in [Tschirpke et al., 2023]). Moreover, we observed heterogeneity in Cdc42 behaviour in these GTPase assays: some Cdc42 constructs showed a quadratic rate increase with Cdc42 concentration, others exhibited a linear one (S4). As our goal was to explore Cdc42 - effector interactions, we used this general phenomenological description (Eq. 1) to fit the Cdc42 data. We remain cautious from deriving any concluding from this data about Cdc42 dimerisation.

For Cdc42 used in this study we observed an almost linear rate increase with Cdc42 concentration, with a small quadratic contribution (Fig. 3a, Tab. 1). Given that data obtained from these GTPase assays is generally reproducible (S5 and [Tschirpke et al., 2023]), we use these rates as a baseline Cdc42 activity to fit all other data.

The GEF Cdc24 is active at sub-μM concentrations and increases Cdc42 activity non-linearly

We next investigated how Cdc24 affects Cdc42 GTPase activity. Cdc24 is a known GEF, increasing the speed of the GDP release step. In agreement with previous studies [Rapali et al., 2017], sub-μM concentrations of Cdc24 substantially boost Cdc42's GTPase activity (Fig. 3b): the rate-contribution of Cdc24 is two orders of magnitude greater than those of Cdc42 alone ($K_{3,Cdc24} \gg K_1, K_2$ (in presence of 1μM of each protein) (Fig. 3e, Tab. 2)). We find that Cdc24's effect increases non-linearly with its concentration (Fig. 3b), which could be explained by Cdc24 di- or oligomerisation: Cdc24 has the capability to oligomerise via its DH domain [Mionnet et al., 2008]. Dimers and oligomers could have an increased GEF activity through releasing Cdc24 from its self-inhibited state [Shimada et al., 2004]. For Cdc24 concentrations used in this assay, we did not observe a saturation of Cdc24's effect on Cdc42 GTPase cycling (S6).

In conclusion, the GEF Cdc24 exhibits activity at sub-μM concentrations and demonstrates a non-linear rate increase on the Cdc42 GTPase activity, possibly due to oligomerisation.

The effect of the GAP Rga2 on the Cdc42 GTPase cycle saturates at μM concentrations and is weaker than that of the GEF

So-far, the GAP activity of Rga2 was only studied using its GAP domain [Smith et al., 2002]. We here use full-size protein. In presence of 1 μM Cdc42, the overall GTP hydrolysis rate of Cdc42 increases with the Rga2 concentration up until about 0.5 μM Rga2, after which it saturates (Fig. 3c). We use our model to fit the regime that can be approximated with a linear rate increase (0-0.5 μM, Fig. 3c blue line). In this regime the rate contribution of Rga2 is about double of that of Cdc42 and an order of magnitude smaller than the effect of Cdc24 (in presence of 1μM of each protein) (Fig. 3e, Tab. 2)

For modelling the GTP decrease in our assay we so-far course-grained the GTPase cycle into one step (S1). If we now model the GTPase steps individually, at a Rga2:Cdc42 ratio of about 1:2 the rate-limiting step is no longer the GTP hydrolysis but the GDP release, thus leading to a saturation of the effect of Rga2 (Fig. 3c green line, model described in S1). Our data on Cdc24 - a protein enhancing GDP release by Cdc42 - shows a large effect of Cdc24 on Cdc42's GTPase activity (Fig. 3b), supporting the notion that the saturation in the Rga2 data is because the GDP release becomes the rate-limiting step.

However, it is also possible that the saturation is due to Rg2 oligomerisation: At some Rga2 concentration Rga2 di- or multimers could form. The amount of multimers would increase with increasing Rga2 concentration, until an equilibrium between monomers and multimers is reached. If the GAP-activity of these multimers is significantly lower than the GAP-activity of remaining monomers, the GAP-activity of the entire Rga2 pool would saturate once equilibrium is reached. The effect of Rga2 oligomerisation would be in stark contrast to Cdc24 oligomerisation: Cdc24 oligomers exhibit an increased GEF activity, whereas Rga2 oligomers show a reduced GAP activity. Overall, a model based on Rga2 oligomerisation fits the Rga2 data less well. We believe that the saturation of the GTPase cycle boosting effect of Rga2 due to oligomerisation is therefore less likely, but we can not exclude it.

Proteins that are not part of the yeast polarity network might affect Cdc42 GTPase cycling *in vitro*

Next, we assessed if proteins that are not part of the yeast polarity protein system (BSA, Casein), and considered inert, affect Cdc42 GTPase cycling *in vitro*. Surprisingly, we found that both increased the overall GTP hydrolysis cycling rate of Cdc42 (Fig. 3d and S7 Fig. 1); the rate contributions of both BSA and Casein ($K_{3,BSA}$, $K_{3,Casein}$) are in the same order of magnitude as those of Cdc42, but smaller than those of Rga and Cdc24 (in presence of 1μM of each protein) (Fig. 3e and S7 Fig. 1). We observed the same trend for the human Ras GTPase; additions of Casein increased the overall GTP hydrolysis cycling rate (with $K_{3,Casein} \approx K_2(Ras)$ (in presence of 1μM of each protein), S9). Ras showed a smaller activity than Cdc42, and the effect of Casein on Ras was smaller than that on Cdc42 (S7 Fig. 1). In absence of a GTPase, BSA and Casein did not lead to hydrolysed GTP (S7 Fig. 2), showing that they do not cause GTP hydrolysis themselves and that they do not affect any downstream processes of the assay. The BSA and Casein concentrations used here (0-5μM) are also far below concentrations where crowding effects are expected [Chebotareva et al., 2004]. We suspect that through sticking to reaction chamber walls BSA/Casein increase the effective GTPase concentration in the assay, thus causing an increase in the overall GTP hydrolysis rate (S7). But given that the chemical reaction pathway of how GTPases hydrolyse GTP is still debated [Calixto et al., 2020], we also can not exclude a rate-affecting interaction between the GTPase and BSA/Casein (discussed in S7). We use the effect sizes of BSA and Casein as a control to account for any effects due to the assay process and/or non-specific interactions between the GTPase and an effector protein. The effect of both Rga2 and Cdc24 was at least an order of magnitude above that of BSA (in presence of 1μM of each protein) (Tab. 2), verifying that it is Rga2- and Cdc24-specific.

Cdc24 and Rga2 synergistically increase the GTPase activity of Cdc42

So-far, we analysed the individual effect of the GEF Cdc24 and GAP Rga2 on the GTPase activity of Cdc42. We now investigate their combined effect on Cdc42 (Fig. 4a). We fit the assay data, containing various concentrations of Cdc24 and Rga2, alone with Cdc42 and combined, with

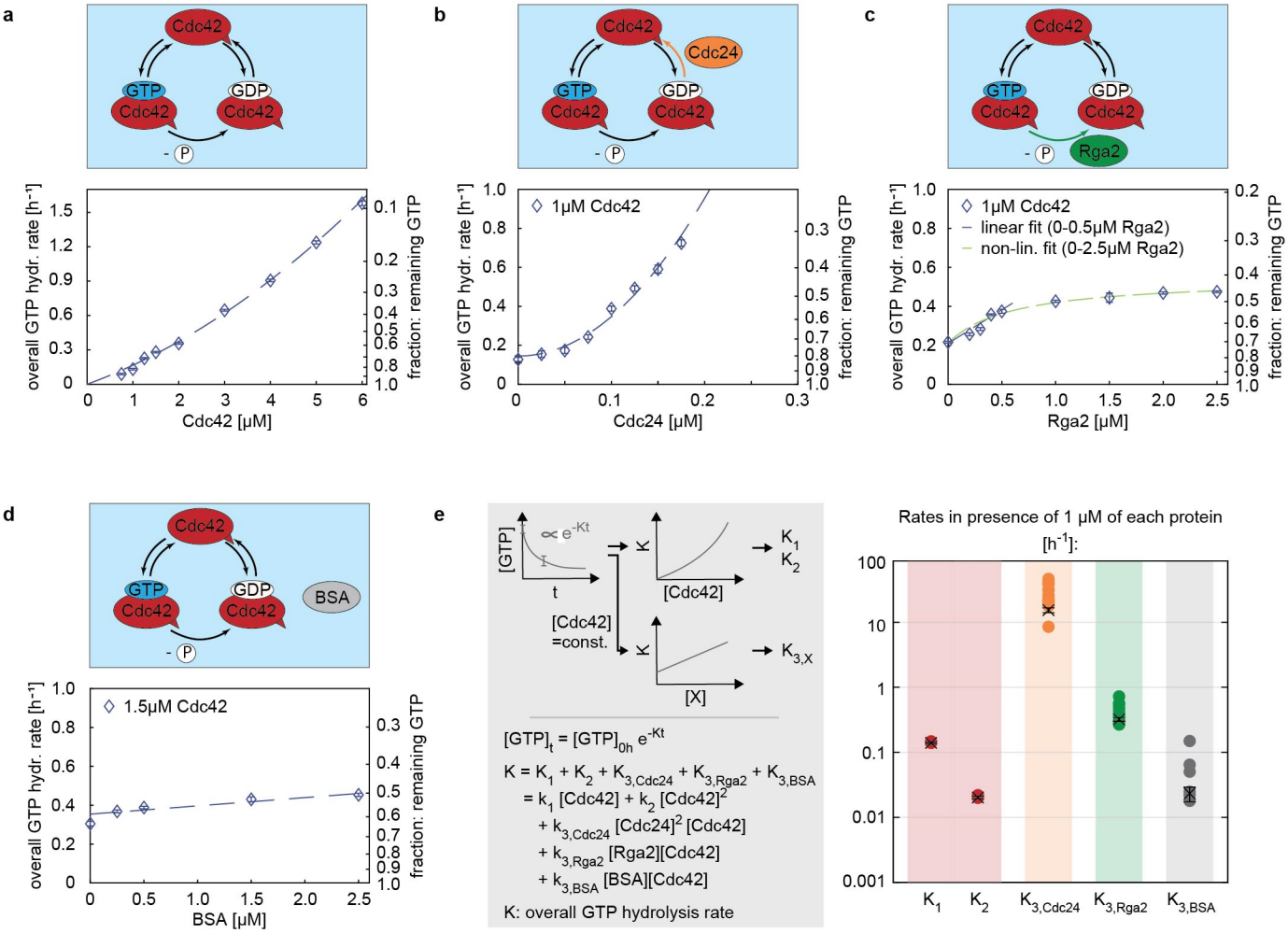

Figure 3. The polarity proteins Cdc24 and Rga2 boost Cdc42's GTPase acitivty with distinct concentration-dependent profiles: Cdc24, even at sub-μM concentrations, enhances Cdc42's GTPase activity in a quadratic fashion. Rga2 has a comparatively small effect, which saturates at 0.5 μM. (a) The overall GTP hydrolysis rate (K) of Cdc42 scales non-linearly with the Cdc42-concentration. (b) Cdc24 boosts the GTPase activity of Cdc42 in a quadratic fashion and is active even at sub-μM concentrations. (c) Rga2 has a small GTPase-activity enhancing effect which saturates. In the regime of 0 - 0.5 μM Rga2 it can be approximated by a linear function. The entire concentration-dependence requires a more elaborate model. Both fitting models are described in S1. (d) Bovine serum albumin (BSA), even though it is not part of the polarity protein network and has no known interactions with Cdc42, also enhances it's GTPase cycling slightly. This effect could be due to (1) unknown non-specific interactions or (2) because it coats to the reaction chamber wall, preventing Cdc42 from binding, thus increasing the active Cdc42 concentration in the reaction. (e) Illustration of the data processing and fitting model and summary of the obtained rates: the effect of Cdc24 on the the GTPase cycling rate of Cdc42 is an order of magnitude greater than that of Rga2, which in turn has a greater effect than BSA. The values shown refer to the rate values in presence of 1 μM of each protein, e.g. '$K_{3,Cdc24}$' refers to '$k_{3,Cdc24}$ [Cdc24]^2 [Cdc42]' with [Cdc42]=[Cdc24]=1 μM. (a-e) Crosses with error bars represent the weighted mean and the standard error of the mean (S2), and filled circles show individual measurements. An overview of all rate values is given in Tab. 1, Tab. 2 and S9.

$$
\begin{gathered}
[\mathrm{GTP}]_t = [\mathrm{GTP}]_{0h} \exp(-Kt) \\
\text{using } [\mathrm{GTP}]_{0h} = 1 \\
\text{and } K = K_1 + K_2 + K_{3,Cdc24} + K_{3,Rga2} + K_{3,Cdc24,Rga2} \\
K = k_1[\mathrm{Cdc42}] + k_2[\mathrm{Cdc42}]^2 + k_{3,Cdc24}[\mathrm{Cdc24}]^2[\mathrm{Cdc42}] + k_{3,Rga2}[\mathrm{Rga2}][\mathrm{Cdc42}] + k_{3,Cdc24,Rga2}[\mathrm{Cdc24}]^2[\mathrm{Rga2}][\mathrm{Cdc42}]
\end{gathered}
\tag{2}
$$

Here $K_{3,Cdc24}$ and $K_{3,Rga2}$ stand for the individual rate contributions of the GEF and GAP, and $K_{3,Cdc24,Rga2}$ is the interaction term. A positive interaction term represents synergy between the GEF and GAP, a negative value represents inhibition. If the term is zero, both proteins would not affect each other. To keep the analysis simple, we only used Rga2 concentrations of the linear regime (0-0.5μM).

In presence of both Cdc24 and Rga2, the GTPase activity of Cdc42 increases drastically (Fig. 4a). In our model the effectors contribute to the overall GTP hydrolysis rate K of Cdc42 through three terms: $K_{3,Cdc24}$, $K_{3,Rga2}$, and $K_{3,Cdc24,Rga2}$. $K_{3,Cdc24}$ and $K_{3,Rga2}$ represent the rate contribution of Cdc24 and Rga2 alone. They are in the three-protein mixture (Cdc42 + Cdc24 + Rga2) the same as when Cdc42 was incubated with one effector alone (Cdc42 + Cdc24, or Cdc42 + Rga2) (Fig. 4d). Importantly, the interaction term $K_{3,Cdc24,Rga2}$ is the dominating term: it is an order of magnitude larger than the Cdc24 rate $K_{3,Cdc24}$ and two orders or magnitude larger than the Rga2 rate $K_{3,Rga2}$ ($K_{3,Cdc24,Rga2} \gg K_{3,Cdc24} \gg K_{3,Rga2}$ (in presence of 1μM of each protein)) (Fig. 4d, Tab. 3). Cdc24 and Rga2 together have a vastly bigger effect than alone (which is especially true for Rga2).

To ensure the observed synergy is due to Cdc24 and Rga2 specific interactions, we also conducted assays with Cdc42, Cdc24, BSA (Fig. 4b), and Cdc42, Rga2, BSA mixtures (Fig. 4c). Again, the contributions of the individual proteins were about the same as before (Fig. 4d, Tab. 3). The interaction term of Cdc24 and BSA was in order of magnitude as the individual contribution of Cdc24 ($K_{3,Cdc24} \approx K_{3,Cdc24,BSA}$ (in presence of 1μM of each protein)) and Rga2 and BSA showed no interaction ($K_{3,Cdc24,BSA} \approx 0$)[1]. We observed the same trends when BSA was exchanged for Casein (S8). If the effect of BSA/Casein is only an artefact of the assay, this data confirms that the synergy between Cdc24 and Rga2 is due to protein-specific interactions; the Cdc24-Rga2 interaction term is an order of magnitude larger than those between BSA/Casein and Cdc24 or Rga2. If BSA/Casein are sticking to reaction chamber walls, they can increase the effective concentration of Cdc42 and Cdc24/Rga2 in the assay. Given that Cdc24 had a strong and Rga2 had a weak effect on Cdc42, an increase in the effective Cdc24 concentration results in a significant increase of the overall GTP hydrolysis rate (leading to a positive $K_{3,Cdc24,BSA}$), whereas an increase in the effective Rga2 concentration has almost no observable effect ($K_{3,Rga2,BSA} \approx 0$). It is also possible that BSA/Casein interact with the Cdc42-Cdc24 complex, or affect the GTP hydrolysis step in such a way that this effect is no longer observable once Rga2 is added.

In conclusion, the data reveals that Rga2 and Cdc24 boost the Cdc42 GTase activity synergistically, with the synergy dominating the reaction speed.

[1]The fit quality for the Cdc42-Rga2-BSA data was significantly lower than for all other data sets ($R^2 \approx 0.5$). Hence, we remain cautious drawing conclusions from this data.

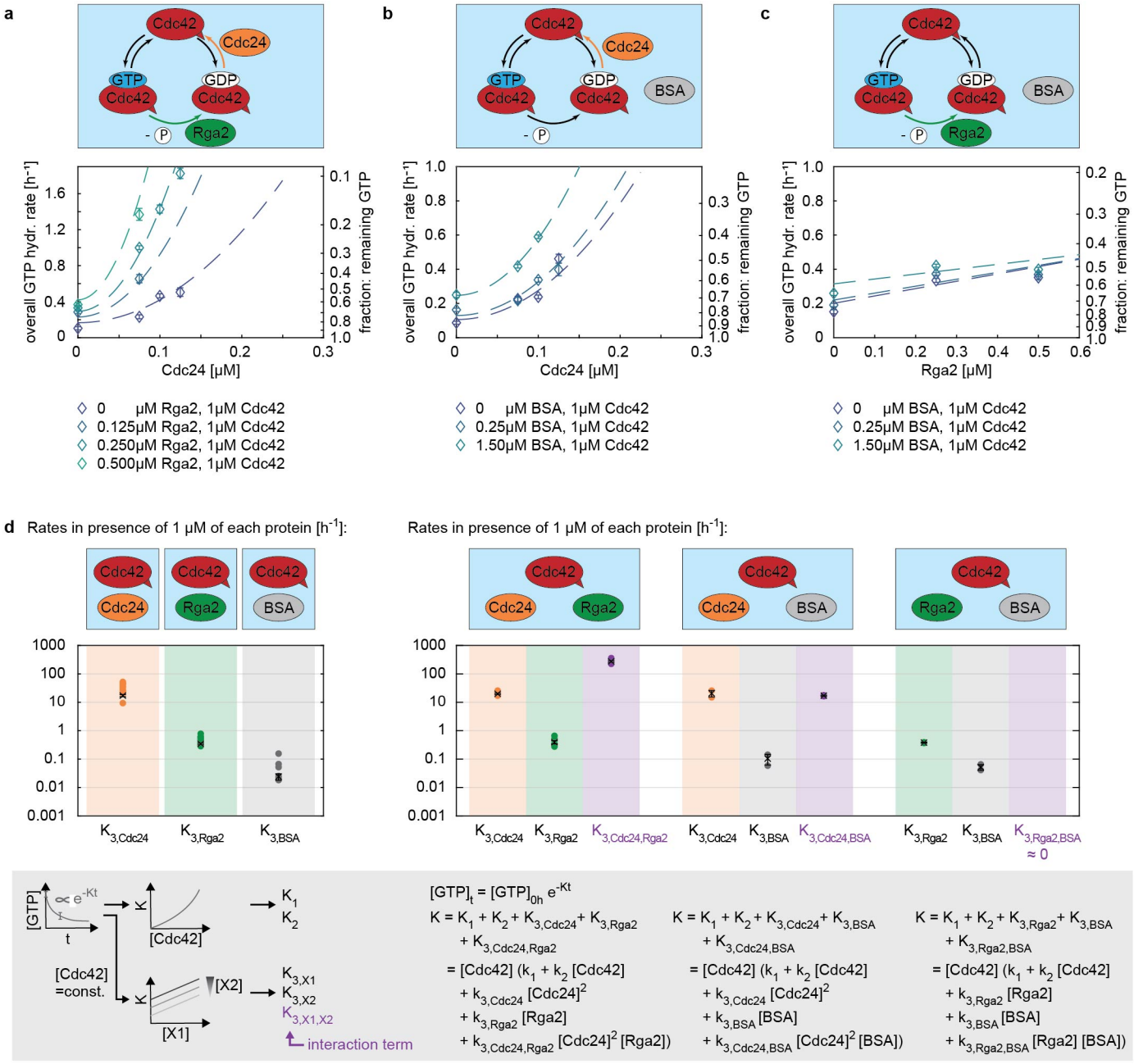

Figure 4. Cdc24 and Rga2 synergistically boost GTPase cycling of Cdc42. Increase in the overall GTP hydrolsis cycling rate (K) of Cdc42 in presence of (a) Cdc24 and Rga2, (b) Cdc24 and BSA, and (c) Rga2 and BSA. (d) Illustration of the data processing and fitting model and summary of the obtained rates obtained in the three-protein assay (right) in comparison to those of the two-protein assay (left): In three-protein assays the rate contribution of the individual proteins is comparable to those obtained in the two-protein assay. Additionally, an interaction rate is obtained (shown in purple). This rate is huge in the case of Cdc42-Cdc24-Rga2 mixtures, indicating a strong synergy between Cdc24 and Rga2. In the case of Cdc42-Cdc24-BSA and Cdc42-Rga2-BSA mixtures, the interaction rate is comparable to the Cdc24 contribution/zero, indicating a weak/ almost no synergy. This effect could be due to non-specific protein-protein binding or because BSA coats to the reaction chamber wall, preventing the other proteins from binding, thus increasing the active concentration in the reaction. The values shown refer to the rate values in presence of 1μM of each protein, e.g. '$K_{3,Cdc24}$' refers to '$k_{3,Cdc24}$ [Cdc24]^2 [Cdc42]' with [Cdc42]=[Cdc24]=1 μM. Crosses with error bars represent the weighted mean and the standard error of the mean (S2), and filled circles show individual measurements. An overview of all rate values is given in Tab. 3 and S9.

Table 1. GTP hydrolysis cycling rates k_1 and k_2 of Cdc42.

	k_1 [μM^{-1} h^{-1}]	k_1 std. err. [μM^{-1} h^{-1}]	k_2 [μM^{-2} h^{-1}]	k_2 std. err. [μM^{-2} h^{-1}]
pooled estimate (n=2)	0.148	0.004	0.021	0.001

Table 2. Interaction rates $k_{3,X}$ of Cdc42 - effector protein mixtures. *: unit in case of X=Cdc24: [μM^{-3} h^{-1}].

	Effector protein X	$k_{3,X}$ [μM^{-2} h^{-1}] *	$k_{3,X}$ std. err.
pooled est. (n=16)	Cdc24	17.239	1.524
pooled est. (n=14)	Rga2	0.345	0.024
pooled est. (n=6)	BSA	0.024	0.006

Table 3. Cdc42 - effector protein X interaction rates k_{3,X_1}, k_{3,X_2}, and k_{3,X_1,X_2}. *: unit in case of X_1=Cdc24: [μM^{-3} h^{-1}]. **: unit in case of X_1=Cdc24: [μM^{-4} h^{-1}].

	Effector protein X_1	Effector protein X_2	k_{3,X_1} [μM^{-2} h^{-1}] *	k_{3,X_1} std. err.	k_{3,X_2} [μM^{-2} h^{-1}]	k_{3,X_2} std. err.	k_{3,X_1,X_2} [μM^{-3} h^{-1}] **	k_{3,X_1,X_2} std. err.
pooled est. (n=6)	Cdc24	Rga2	19.898	1.143	0.395	0.051	275.343	19.940
pooled est. (n=2)	Cdc24	BSA	20.746	5.405	0.104	0.042	17.101	0.692
pooled est. (n=2)	Rga2	BSA	0.380	0.011	0.052	0.012	-0.073	0.008

Discussion

Here, we investigated how GEFs and GAPs, solely and in combination, regulate Cdc42 GTPase cycling.

We used an assay that determines the overall GTP hydrolysis rate through the amount of remaining GTP after several numbers of GTPase cycles. An advantageous aspect of this assay is that interactions between proteins that affect distinct GTPase cycle steps, i.e. GEFs and GAPs, can be assessed. A potential drawback is that during the GTPase reaction, the amount of remaining GTP, and thus the amount of GTP that can be hydrolysed by the GTPase, drops significantly (Fig. 3, 4). *In vivo* GTP concentrations are high and regimes with an excess of GDP are unlikely to be reached. Thus, the rates measured here can not be transferred one to one to the *in vivo* situation. We expect that the effect of the GEF is prolonged and the effect of the GAP is weaker in this assay compared to *in vivo*. Given the orders of magnitude big differences between rate contributions of GTPase, GEF, GAP, and GEF-GAP interaction (Fig. 4d), the effects will very likely still be in affect *in vivo*.

We showed the concentration-dependent impact of Cdc24 (GEF) and Rga2 (GAP) on Cdc42 GTPase cycling. Both proteins exhibited a vastly different behaviour, with the effect of Rga2 being comparatively small to that of Cdc24, which is active even at sub-μM concentrations. Our data suggests that overall GTP hydrolysis rate K does not depend linearly on the Cdc24 concentration but is better approximated by a quadratic term (Fig. 3b), suggesting cooperativity. This could be facilitated through Cdc24 dimers and oligomers that exhibit an increased GEF activity. This hypothesis is in partial agreement with previous findings: Mionnet *et al.* showed that Cdc24 has the capability to oligomerise via its DH domain [Mionnet et al., 2008]. However, truncated Cdc24 constructs consisting only of Cdc24's DH and PH domain exhibited GEF activity that was not changed when oligomerisation was inhibited or amplified [Mionnet et al., 2008]. These findings exclude that these truncated Cdc24 oligomers exhibit an increased GEF activity. However, we believe it is necessary to be cautious when applying these findings

to full-length Cdc24: Other domains that are not directly involved in oligomerisation or GEF function can still affect these properties. Next, Mionnet *et al.* induced a heightened oligomerisation state to the truncated Cdc24 construct by adding an artificial oligomerisation domain, which could be triggered to oligomerise through the addition of a chemical. We find it questionable if the GEF activity of these oligomeric truncated Cdc24 constructs relates to the GEF activity of oligomeric full length Cdc24: A heightened GEF activity of Cdc24 dimers could be facilitated by Cdc24's C-terminal PB1-domain, which has been suggested to reduce Cdc24's GEF activity through intramolecular interactions [Shimada et al., 2004], and is absent in the truncated Cdc24 constructs. Cdc24 oligomerisation could interfere with this self-interaction and thereby increase the proteins GEF activity.

We also investigated the GAP-effect of full-size Rga2, of which so-far only its GAP domain was probed *in vitro* [Smith et al., 2002]. Our data revealed that the GAP-effect of Rga2 saturates at about half of the Cdc42 concentration present (Fig. 3c). The saturation could originate from kinetics of the GTPase cycle steps: when GTP hydrolysis is slow (compared to GDP release), the overall rate (K) increases linearly with increasing hydrolysis rate (and thus increasing Rga2 concentration). At some point, hydrolysis becomes sufficiently fast that GDP release is rate-limiting, such that the overall rate reaches a maximum. Another possible interpretation is that Rga2 starts to form self-inhibitory di- or multimers at elevated concentrations.

We examined how the GEF Cdc24 and GAP Rga2 together affect Cdc42 GTPase cycling. We found that Cdc24 and Rga2 exhibit a large synergy, which is the mayor contributor to the overall GTP hydrolysis rate. We only used Rga2 and Cdc24 concentrations below saturation (i.e. in which neither the GTP hydrolysis nor the GDP release step seem rate limiting), suggesting that the synergy occurs due to proteins enhancing each others effect. The GAP-effect of Rga2 was in contrast to the GEF-effect of Cdc24 comparatively weak. The large synergy between the two proteins could indicate that Rga2's full effect on Cdc42 is not be apparent when studied in isolation, but only becomes noticeable in conjunction with Cdc24 and potentially other proteins. This raises the question which other proteins, who's effect is currently thought to be understood, take on another or quantitatively different effect, in presence of another protein. It would further be interesting to investigate whether Rga1 and Bem2, other GAPS genetically interacting with Cdc24, show similar effects in conjunction with Cdc24, or if this is Rga2 specific. Our data shows a synergy between Rga2 and Cdc24, but does not reveal how this synergy occurs - does Cdc24 boost Rga2's GAP activity, does Rga2 boost Cdc24's GEF activity, or do both positively affect each other? Cdc24's GEF activity can be further enhanced (by the scaffold Bem1 [Rapali et al., 2017]), but this effect was found to be rather weak. Given that the GAP-effect of Rga2 was smaller than Cdc24's GEF-effect, we propose the effect sizes observed here are more likely explained by a GAP-boosting affect of Cdc24. Cdc24 affecting Rga2's GAP activity requires that Cdc24 and Rga2 bind to each other. Does Cdc24 bind to Rga2? Interaction studies showed that a direct or mediated interaction between Cdc24 and Rga2 occurs [Chollet et al., 2020]. Cdc24 and Rga2 share 11 common binding partners (Isw1, Scc2, Rsr1, Ccr4, Boi1, Boi2, Ent2, Ebp2, Bem1, Hek2, Dhh1) [BioGRID, 2023a, BioGRID, 2023b], which could mediate the Cdc24 - Rga2 interaction. Among those common binding partners, the scaffold Bem1 is an obvious candidate for mediating Cdc24 - Rga2 binding. However, the Cdc24 - Rga2 interaction also occurs cells lacking Bem1 [Chollet et al., 2020]. Based on the existing data we can not estimate whether Cdc24 and Rga2 bind directly and thus if Cdc24 can enhance Rga2's GAP activity through direct physical interactions.

How does our data integrate with existing knowledge of polarity establishment? We found that Rga2 shows a rather low GAP-effect which saturates at low µM concentrations. The emergence of Rga2's low GAP activity could be the result of epistasis - a phenomenon where the effect of one gene masks or modifies the effect of another gene: Cdc24 is an essential gene product in *S. cerevisae* and highly conserved in the fungal tree [Diepeveen et al., 2018], making it a persistent player in the polarity network. Mutations in Rga2 that only reduce its sole GAP activity would be permitted and masked by Rga2's synergistic effect with Cdc24, and could emerge without reducing the organism's fitness. Rga2 is only one of four GAPs of Cdc42 (among Rga1, Bem2, and Bem3). It was suggested that each GAP plays a distinct role in Cdc42 regulation, of which the level of GAP activity could be a part of [Smith et al., 2002]. In addition to the general strength of GAP activity, our data on Rga2 suggests that (1) the concentration-dependent profile of the GAP activity, and (2) synergies with other regulator factors could be other distinguishing factors. *In vitro* analysis of other GAPs (their concentration-dependent GAP activity with and without other regulators) would help to clarify if and how different GAP-activities contribute to different roles of GAPs in *S. cerevisae*.

Our data exemplifies non-linearities of Cdc42 GTPase cycle regulation: (1) the overall GTP hydrolysis rate of Cdc42 increases quadratically with Cdc24 concentration. (2) the GEF Cdc24 and GAP Rga2 exhibit synergy. Both non-linearities could contribute to establishing polarity through creating regimes of high and low Cdc42 activity: (1) Temporal regulation of Cdc42 activity: *In vivo*, the timed release of Cdc24 from the nucleus (thus suddenly increasing the effective Cdc24 concentration) is known to be part of the polarity trigger [Shimada et al., 2000]. We suspect that the non-linear increase of the overall GTP hydrolysis rate of Cdc42 with Cdc24 concentration is a mechanistic element of Cdc24's function *in vivo*: once Cdc24 gets released from the nucleus, the GTPase cycling speed of Cdc42 increases strongly and suddenly (due to its non-linear dependence on Cdc24 concentration). With the release of Cdc24 from the nucleus, cells can quickly transition from a regime of low GTPase activity of Cdc42 (before the release of Cdc24) to a regime of high GTPase activity of Cdc42 (after the release of Cdc24). The sudden change in Cdc42's GTPase cycling speed could initiate polarity establishment. (2) Spatial regulation of Cdc42 activity: The synergistic regulation of Cdc42's GTPase activity through GEFs and GAPs is a resourceful and advantageous way of regulation; if regulatory factors have a synergistic interplay, wide ranges of up-regulation can be achieved through a small amount of components. This synergy also implies that Cdc42 has a significantly higher GTPase activity at the polarity spot, where it is surrounded by many effector proteins, that also regulate each other. We suspect the strong up-regulation at the site of bud emergence and the rather low baseline activity at other sites to have a cellular purpose, and imagine it is contributing to Cdc42 accumulation.

Beyond its impact on our understanding of the yeast system, our findings may also apply to other eukaryotes: Cdc42 is highly conserved among eukaryotes, and plays a central role in polarity establishment in many of these [Nelson, 2003, Etienne-Manneville, 2004, Thompson, 2013, Diepeveen et al., 2018]. We imagine that the principles of its regulation are also conserved there, and suspect that synergies between GEFs and GAPs also occur in these systems.

Materials and Methods

Plasmid construction

Genes of interest (Cdc42, Rga2) were obtained from the genome of *Saccharomyces cerevisiae* W303 and were amplified through PCR. The target vector was also amplified through PCR. Additionally, each PCR incorporated a small homologous sequences needed for Gibson assembly [Gibson et al., 2009]. After Gibson assembly, the resulting mixture was used to transform chemically competent Dh5α and BL21 DE::3 pLysS cells and plated out onto a Petri dish containing Lysogeny broth agar and the correct antibiotic marker. The primers used for each PCR can be found in S11. Gibson assembly resulted in plasmids pRV007 and pRV014. The amino acid sequences of the proteins used in this publication are stated in S10 and their design is discussed in detail in [Tschirpke et al., 2023].

Buffer composition

If not mentioned otherwise, buffers are of the composition stated in Tab. 5.

Table 4. List of protein constructs/plasmids used throughout this publication.

Plasmid	Description	Source
pET28a-His-mcm10-Sortase-Flag	template for pRV007, pRV014	received from N. Dekker (TU Delft), based on pBP6 [Douglas and Diffley, 2016]
pRV007	Cdc42	this work
pRV014	Rga2	this work
pDM272	Cdc24	received from D. McCusker (University of Bordeaux) (published in [Rapali et al., 2017])

Table 5. Buffer composition.

Buffer	Composition
Lysis buffer	50 mM Tris-HCl (pH=8.0), 1 M NaCl, 5 mM imidazole, 1 mM 2-mercaptoethanol (Sigma Aldrich), supplemented with EDTA-free Protease inhibitor cocktail (Roche) and 1 mM freshly prepared PMSF.
His-AC washing buffer	50 mM Tris-HCl (pH=8.0), 1 M NaCl, 5 mM imidazole, 1 mM 2-mercaptoethanol (Sigma Aldrich).
His-AC elution buffer	50 mM Tris-HCl (pH=8.0), 100 mM NaCl, 500 mM imidazole, 1mM 2-mercaptoethanol (Sigma Aldrich).
SEC buffer	50 mM Tris-HCl (pH=7.5), 100 mM NaCl, 10 mM $MgCl_2$, 1 mM 2-mercaptoethanol (Sigma Aldrich).

Protein expression and purification

Cdc42 (pRV007) was expressed in Bl21::DE3 pLysS cells. Cells were grown in Lysogeny broth at 37°C until an OD_{600} of 0.7. The expression was induced through addition of 1.0 mM IPTG, after which cells were grown for 3 h at 37°C. Cells were harvested through centrifugation. Cell pellets were resuspended in lysis buffer and lysed with a high pressure homogenizer (French press cell disruptor, CF1 series Constant Systems) at 4°C, using 5-10 rounds of exposing the sample to pressurisation. The cell lysate was centrifuged at 37000× g for 30 min and the supernatant was loaded onto a HisTrap™ excel column (Cytiva). After several rounds of washing with His-AC washing buffer, the protein was eluted in a gradient of His-AC washing buffer and His-AC elution buffer. The protein as dialysed twice in SEC buffer. After the addition of 10% glycerol, samples were flash frozen in liquid nitrogen and kept at -80°C for storage.

The **Cdc24 (pDM272)** expression and purification is, with modifications, based on the protocol described previously [Rapali et al., 2017]. Cdc24 was expressed in Bl21::DE3 pLysS cells. Cells were grown in Lysogeny broth at 37°C until an OD_{600} of 0.7. The expression was induced through addition of 0.2 mM IPTG, after which cells were grown for 18 h at 18°C. Cells were harvested through centrifugation. Cell pellets were resuspended in lysis buffer and lysed with a high pressure homogenizer (French press cell disruptor, CF1 series Constant Systems) at 4°C, using 5-10 rounds of exposing the sample to pressurisation. The cell lysate was centrifuged at 37000× g for 30 min and the supernatant was loaded onto a HisTrap™ excel column (Cytiva). After several rounds of washing with His-AC washing buffer, the protein was eluted in a gradient of His-AC washing buffer and His-AC elution buffer. The sample was further purified by size exclusion chromatography using SEC buffer and a HiPrep 16/60 Sephacryl S-300 HR (Cytiva) column. Fractions containing full-size protein were concentrated using Amicon®Ultra 4 mL centrifugal filters (Merck). After the addition of 10% glycerol, samples were flash frozen in liquid nitrogen and kept at -80°C for storage.

Rga2 (pRV014) was expressed in Bl21::DE3 pLysS cells. Cells were grown in Lysogeny broth at 37°C until an OD_{600} of 0.7. The expression was induced through addition of 0.2 mM IPTG, after which cells were grown for 18 h at 10°C. Cells were harvested through centrifugation. Cell pellets were resuspended in lysis buffer (supplemented with 0.1% Tween-20 (Sigma Aldrich), 0.1% NP-40 (Thermo Fischer Scientific), and 0.1% Triton-X-100 (life technologies (now: Invitrogen))) and lysed with a high pressure homogenizer (French press cell disruptor, CF1 series Constant Systems) at 4°C, using 5-10 rounds of exposing the sample to pressurisation. The cell lysate was centrifuged at 37000× g for 30 min and the supernatant was loaded onto a HisTrap™ excel column (Cytiva). After several rounds of washing with His-AC washing buffer (supplemented with 0.1% Tween-20 (Sigma Aldrich), 0.1% NP-40 (Thermo Fischer Scientific), and 0.1% Triton-X-100 (life technologies (now: Invitrogen))), the protein was eluted in a gradient of His-AC washing buffer and His-AC elution buffer (both supplemented with 0.1% Tween-20 (Sigma Aldrich), 0.1% NP-40 (Thermo Fischer Scientific), and 0.1% Triton-X-100 (life technologies (now: Invitrogen))). The sample was further purified by size exclusion chromatography using SEC buffer and a HiPrep 16/60 Sephacryl S-300 HR (Cytiva) column. Fractions containing full-size protein were concentrated using Amicon®Ultra 4 mL centrifugal filters (Merck). After the addition of 10% glycerol, samples were flash frozen in liquid nitrogen and kept at -80°C for storage.

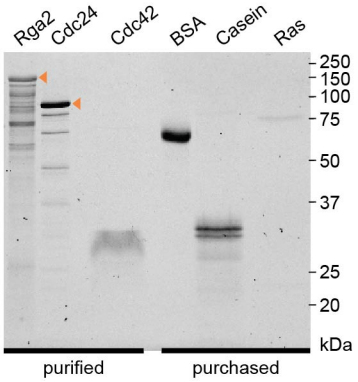

Figure 5. SDS-Page of used proteins. An orange arrow indicates the band of the correct size.

Note on His-affinity chromatography: HisTrap™ excel column (Cytiva) columns bought 2020 or later required a higher amount of imidazole in the lysis and washing buffer that stated in Tab. 5, as indicated by the recommendation 'use 20-40 mM imidazole in sample and binding buffer for highest purity' on the column package. For these columns the amount of imidazole in lysis and His-AC washing buffer was increased to 50 mM.

Casein (C7078, Sigma-Aldrich) was dissolved in SEC buffer. **Bovine serum albumin (BSA)** (23209, Thermo Scientific) was dialysed twice in SEC buffer. **Ras** (human) (553325, EMD Millipore) was diluted in SEC buffer.

All proteins are shown on SDS-Page in Fig. 5.

GTPase activity assay

GTPase activity was measured using the GTPase-Glo™ assay (Promega) following the steps described in the assay manual: in brief, 5 µL protein in SEC buffer (Tab. 5) was mixed with 5 µL of a GTP-solution (10 µM GTP, 50 mM Tris-HCl (pH=7.5), 100 mM NaCl, 10 mM $MgCl_2$, 1 mM 2-mercaptoethanol (Sigma Aldrich), 1 mM dithiothreitol (VWR) in 384-well plates (Corning) to initiate the reaction. The reaction mixture got incubated at 30°C on an Innova 2300 platform shaker (New Brunswick Scientific) (120 rpm), before the addition of 10 µL Glo buffer and another 30 min incubation. The Glo buffer contains a nucleoside-diphosphate kinase that convert remaining GTP to ATP. Addition of 20 µL detection reagent, containing a luciferase/luciferin mixture, makes the ATP luminescent, which was read on a Synergy HTX plate reader (BioTek) in luminescence mode.
This GTPase assay can be sensitive to small concentration differences, especially of effector proteins. To reduce the variability between assays and to increase comparability of different assay sets, 6× proteins stocks were made using serial dilutions (with SEC buffer). The assays were conducted using the same 6× proteins stocks within a few days, during which these stocks were kept at 4°C. For each assay, equivalent volumes of 6× protein stocks were diluted to 2× mixtures (e.g. 10 µL Cdc42 + 20 µL SEC buffer, 10 µL Cdc42 + 10 µL effector protein 1 + 10 µL SEC buffer, 10 µL Cdc42 + 10 µL effector protein 1 + 10 µL effector protein 2, ...). Incubation of 5 µL of this protein mixture with 5 µL of GTP solution, as described above, resulted in the concentrations stated in Fig. 3,4.

Fitting of GTPase data & GTPase model

The amount of remaining GTP correlates with the measured luminescence. Wells without protein ('buffer') were used for the normalisation and represent 0% GTP hydrolysis:

$$[\mathrm{GTP}]_{t_{term.}} = \left(\frac{\text{Lum. protein}}{\text{Lum. buffer}}\right) \tag{3}$$

Wells where no GTP was added showed luminescence values corresponding to <1% remaining GTP. Given the small deviation to 0%, and that GTPase reactions of protein mixtures leading to <5% remaining GTP were excluded from further analysis (S6), we did not normalise the data using luminescence values corresponding to 0% GTP.

Reactions were carried out with three to four replicates (wells) per assay, and the average ('Lum.') and standard error of the mean ('ΔLum.') of each set was used to calculate the amount of remaining GTP at the time of reaction termination and the error of each set:

$$\Delta \text{ remaining GTP} = \sqrt{\left(\frac{\Delta\text{Lum. protein}}{\text{Lum. protein}}\right)^2 + \left(\frac{\Delta\text{Lum. buffer}}{\text{Lum. buffer}}\right)^2} \times \frac{\text{Lum. protein}}{\text{Lum. buffer}} \tag{4}$$

The data was fitted using a GTPase activity model (described in S1). In brief, the GTP decline occurring during the GTPase reaction was fitted with an exponential (S3)

$$[\text{GTP}]_t = [\text{GTP}]_{0h} \exp(-Kt) \tag{5}$$

using $[\text{GTP}]_{0h}$ = 1 and

$$\begin{aligned} K =& k_1 c_{corr}[\text{Cdc42}] + k_2 (c_{corr}[\text{Cdc42}])^2 \\ &+ k_{3,Cdc24} c_{corr}[\text{Cdc42}][\text{Cdc24}]^2 \\ &+ k_{3,Rga2} c_{corr}[\text{Cdc42}][\text{Rga2}] \\ &+ k_{3,BSA} c_{corr}[\text{Cdc42}][\text{BSA}] \\ &+ k_{3,Casein} c_{corr}[\text{Cdc42}][\text{Casein}] \\ &+ k_{3,Cdc24,Rga2} c_{corr}[\text{Cdc42}][\text{Rga2}][\text{Cdc24}]^2 \\ &+ k_{3,Cdc24,BSA} c_{corr}[\text{Cdc42}][\text{BSA}][\text{Cdc24}]^2 \\ &+ k_{3,Cdc24,Casein} c_{corr}[\text{Cdc42}][\text{Casein}][\text{Cdc24}]^2 \\ &+ k_{3,Rga2,BSA} c_{corr}[\text{Cdc42}][\text{Rga2}][\text{BSA}] \\ &+ k_{3,Rga2,Casein} c_{corr}[\text{Cdc42}][\text{Rga2}][\text{Casein}] \end{aligned} \tag{6}$$

or

$$\begin{aligned} K =& k_1 c_{corr}[\text{Ras}] + k_2 (c_{corr}[\text{Ras}])^2 \\ &+ k_{3,Casein} c_{corr}[\text{Ras}][\text{Casein}] \end{aligned} \tag{7}$$

Here K represents the overall GTP hydrolysis rate, and c_{corr} is a variable used to map all factors that lead to variations between GTPase assays onto the Cdc42 concentration (S5).

The pooled estimates of rates k_1, k_2, and k_3 were determined through weighting their standard error, as described in S2.

Acknowledgements

We thank F. van Opstal and R. van der Valk for experimental assistance, F. Shamsi and S. Farooq for their pioneering work of GTPase activity by Cdc42 and its regulators, and M. Depken for careful reading of the manuscript. We thank D. McCusker (University of Bordeaux) for the plasmid pDM272 and N. Dekker (TU Delft) for the plasmid pET28a-His-mcm10-Sortase-Flag.

Contributions

S. Tschirpke: Conceptualization, Methodology, Investigation, Formal analysis, Validation, Writing - Original Draft, Writing - Review & Editing, Visualization, Project administration. **W. K.-G. Daalman:** Conceptualization, Methodology, Investigation, Software, Formal analysis, Validation. **L. Laan:** Conceptualization, Methodology, Investigation, Writing - Review & Editing, Funding acquisition, Project administration.

Funding

L. Laan gratefully acknowledges funding from the European Research Council under the European Union's Horizon 2020 research and innovation programme (grant agreement 758132) and funding from the Netherlands Organization for Scientific Research (Nederlandse Organisatie voor Wetenschappelijk Onderzoek) through a Vidi grant (016.Vidi.171.060).

References

[BioGRID, 2023a] BioGRID (2023a). https://thebiogrid.org/31724/table/saccharomyces-cerevisiae-s288c/cdc24.html.

[BioGRID, 2023b] BioGRID (2023b). https://thebiogrid.org/32438/table/saccharomyces-cerevisiae-s288c/rga2.html.

[Bos et al., 2009] Bos, J., Rehmann, H., and Wittinghofer, A. (2009). GEFs and GAPs: Critical Elements in the Control of Small G Proteins. *Cell*, 16(3):374–383.

[Calixto et al., 2020] Calixto, A. R., Moreira, C., and Kamerlin, S. C. L. (2020). Recent advances in understanding biological gtp hydrolysis through molecular simulation. *ACS Omega*, 5(9):4380–4385.

[Caviston et al., 2002] Caviston, J. P., Tcheperegine, S. E., and Bi, E. (2002). Singularity in budding: A role for the evolutionarily conserved small GTPase Cdc42p. *Proceedings of the National Academy of Sciences of the United States of America*, 99(19):12185–12190.

[Chebotareva et al., 2004] Chebotareva, N. A., Kurganov, B. I., and Livanova, N. B. (2004). Biochemical Effects of Molecular Crowding. *Biochemistry (Moscow)*, 69(11):1239–1251.

[Chiou et al., 2017] Chiou, J.-g., Balasubramanian, M. K., and Lew, D. J. (2017). Cell Polarity in Yeast. *Annual Review of Cell and Developmental Biology*, 33:77–101.

[Chollet et al., 2020] Chollet, J., Dunkler, A., Bauerle, A., Vivero-Pol, L., Mulaw, M. A., Gronemeyer, T., and Johnsson, N. (2020). Cdc24 interacts with septins to create a positive feedback loop during bud site assembly in yeast. *Journal of Cell Science*, 133(11).

[Daalman et al., 2020] Daalman, W. K. G., Sweep, E., and Laan, L. (2020). The Path towards Predicting Evolution as Illustrated in Yeast Cell Polarity. *Cells*, 9(12).

[Das et al., 2012] Das, A., Slaughter, B. D., Unruh, J. R., Bradford, W. D., Alexander, R., Rubinstein, B., and Li, R. (2012). Flippase-mediated phospholipid asymmetry promotes fast Cdc42 recycling in dynamic maintenance of cell polarity. *Nature Cell Biology*, 14(3):304–310.

[Diepeveen et al., 2018] Diepeveen, E. T., Gehrmann, T., Pourquié, V., Abeel, T., and Laan, L. (2018). Patterns of conservation and diversification in the fungal polarization network. *Genome Biology and Evolution*, 10(August):evy121–evy121.

[Douglas and Diffley, 2016] Douglas, M. E. and Diffley, J. F. (2016). Recruitment of Mcm10 to sites of replication initiation requires direct binding to the minichromosome maintenance (MCM) complex. *Journal of Biological Chemistry*, 291(11):5879–5888.

[Etienne-Manneville, 2004] Etienne-Manneville, S. (2004). Cdc42–the centre of polarity. *J Cell Sci*, 117(Pt 8):1291–1300.

[Frey et al., 2018] Frey, E., Halatek, J., Kretschmer, S., and Schwille, P. (2018). Protein Pattern Formation. *arXiv:1801.01365 [physics.bio-ph]*, pages 1–17.

[Gao et al., 2011] Gao, J. T., Guimera, R., Li, H., Pinto, I. M., Sales-Pardo, M., Wai, S. C., Rubinstein, B., and Li, R. (2011). Modular coherence of protein dynamics in yeast cell polarity system. *Proceedings of the National Academy of Sciences*, 108(18):7647–7652.

[Gibson et al., 2009] Gibson, D. G., Young, L., Chuang, R. Y., Venter, J. C., Hutchison, C. A., and Smith, H. O. (2009). Enzymatic assembly of DNA molecules up to several hundred kilobases. *Nature Methods*, 6(5):343–345.

[Glazenburg and Laan, 2023] Glazenburg, M. M. and Laan, L. (2023). Complexity and self-organization in the evolution of cell polarization. *Journal of Cell Science*, 136(2):jcs259639.

[Golding et al., 2019] Golding, A. E., Visco, I., Bieling, P., and Bement, W. M. (2019). Extraction of active RhoGTPases by RhoGDI regulates spatiotemporal patterning of RhoGTPases. *eLife*, 8:1–26.

[Goryachev and Leda, 2017] Goryachev, A. B. and Leda, M. (2017). Many roads to symmetry breaking: molecular mechanisms and theoretical models of yeast cell polarity. *Molecular Biology of the Cell*, 28(3):370–380.

[Heij et al., 2004] Heij, C., de Boer, P., Franses, P. H., Kloek, T., and van Dijk, H. K. (2004). *Econometric Methods with Applications in Business and Economics*. Oxford University Press.

[Johnson et al., 2009] Johnson, J. L., Erickson, J. W., and Cerione, R. A. (2009). New Insights into How the Rho Guanine Nucleotide Dissociation Inhibitor Regulates the Interaction of Cdc42 with Membranes. *Journal of Biological Chemistry*, 284(35):23860–23871.

[Johnson et al., 2012] Johnson, J. L., Erickson, J. W., and Cerione, R. A. (2012). C-terminal Di-arginine motif of Cdc42 protein is essential for binding to phosphatidylinositol 4,5-bisphosphate-containing membranes and inducing cellular transformation. *Journal of Biological Chemistry*, 287(8):5764–5774.

[Kang et al., 2010] Kang, P. J., Béven, L., Hariharan, S., and Park, H. O. (2010). The Rsr1/Bud1 GTPase interacts with itself and the Cdc42 GTPase during bud-site selection and polarity establishment in budding yeast. *Molecular Biology of the Cell*, 21(17):3007–3016.

[Lang and Munro, 2022] Lang, C. F. and Munro, E. M. (2022). Oligomerization of peripheral membrane proteins provides tunable control of cell surface polarity. *Biophysical Journal*, 121(23):4543–4559.

[Martin, 2015] Martin, S. G. (2015). Spontaneous cell polarization: Feedback control of Cdc42 GTPase breaks cellular symmetry. *BioEssays*, 37(11):1193–1201.

[Mionnet et al., 2008] Mionnet, C., Bogliolo, S., and Arkowitz, R. A. (2008). Oligomerization regulates the localization of Cdc24, the Cdc42 activator in Saccharomyces cerevisiae. *Journal of Biological Chemistry*, 283(25):17515–17530.

[Nelson, 2003] Nelson, W. J. (2003). Generating polarity in single cells for mitotic division. *Nature*, 433(April):766–774.

[Park and Bi, 2007] Park, H.-O. and Bi, E. (2007). Central Roles of Small GTPases in the Development of Cell Polarity in Yeast and Beyond. *Microbiology and Molecular Biology Reviews*, 71(1):48–96.

[Rapali et al., 2017] Rapali, P., Mitteau, R., Braun, C., Massoni-Laporte, A., Ünlü, C., Bataille, L., Arramon, F. S., Gygi, S. P., and McCusker, D. (2017). Scaffold-mediated gating of Cdc42 signalling flux. *eLife*, 6:1–18.

[Schlecht et al., 2012] Schlecht, U., Miranda, M., Suresh, S., Davis, R. W., and St.Onge, R. P. (2012). Multiplex assay for condition-dependent changes in protein-protein interactions. *Proceedings of the National Academy of Sciences of the United States of America*, 109(23):9213–9218.

[Shimada et al., 2000] Shimada, Y., Gulli, M.-P., and Peter, M. (2000). Nuclear sequestration of the exchange factor Cdc24p by Far1 regulates cell polarity during mating. *Nature Cell Biology*, 2:117–124.

[Shimada et al., 2004] Shimada, Y., Wiget, P., Gulli, M. P., Bi, E., and Peter, M. (2004). The nucleotide exchange factor Cdc24p may be regulated by auto-inhibition. *EMBO Journal*, 23(5):1051–1062.

[Smith et al., 2002] Smith, G. R., Givan, S. A., Cullen, P., and Sprague, G. F. (2002). GTPase-Activating Proteins for Cdc42. *Eukaryotic Cell*, 1(3):469–480.

[Tarassov et al., 2008] Tarassov, K., Messier, V., Landry, C. R., Radinovic, S., Serna Molina, M. M., Shames, I., Malitskaya, Y., Vogel, J., Bussey, H., and Michnick, S. W. (2008). An in vivo map of the yeast protein interactome. *Science*, 320(5882):1465–1470.

[Thompson, 2013] Thompson, B. J. (2013). Cell polarity: Models and mechanisms from yeast, worms and flies. *Development (Cambridge)*, 140(1):13–21.

[Tschirpke et al., 2023] Tschirpke, S., van Opstal, F., van der Valk, R., Daalman, W., and Laan, L. (2023). A guide to the in vitro reconstitution of Cdc42 activity and its regulation. *pre-print available on BioRxiv*.

[Vendel et al., 2019] Vendel, K. J. A., Tschirpke, S., Shamsi, F., Dogterom, M., and Laan, L. (2019). Minimal in vitro systems shed light on cell polarity. *Journal of Cell Science*, 132(4):1–21.

[Wedlich-Soldner et al., 2004] Wedlich-Soldner, R., Wai, S. C., Schmidt, T., and Li, R. (2004). Robust cell polarity is a dynamic state established by coupling transport and GTPase signaling. *Journal of Cell Biology*, 166(6):889–900.

[Wu et al., 2013] Wu, C. F., Savage, N. S., and Lew, D. J. (2013). Interaction between bud-site selection and polarity-establishment machineries in budding yeast. *Philos Trans R Soc Lond B Biol Sci*, 368(1629):20130006.

[Zhang et al., 2001] Zhang, B., Gao, Y., Moon, S. Y., Zhang, Y., and Zheng, Y. (2001). Oligomerization of Rac1 GTPase Mediated by the Carboxyl-terminal Polybasic Domain. *Journal of Biological Chemistry*, 276(12):8958–8967.

[Zhang et al., 1997] Zhang, B., Wang, Z. X., and Zheng, Y. (1997). Characterization of the interactions between the small GTPase Cdc42 and its GTPase-activating proteins and putative effectors: Comparison of kinetic properties of Cdc42 binding to the Cdc42-interactive domains. *Journal of Biological Chemistry*, 272(35):21999–22007.

[Zhang et al., 1999] Zhang, B., Zhang, Y., Collins, C. C., Johnson, D. I., and Zheng, Y. (1999). A built-in arginine finger triggers the self-stimulatory GTPase- activating activity of Rho family GTPases. *Journal of Biological Chemistry*, 274(5):2609–2612.

[Zhang and Zheng, 1998] Zhang, B. and Zheng, Y. (1998). Negative regulation of Rho family GTPases Cdc42 and Rac2 by homodimer formation. *Journal of Biological Chemistry*, 273(40):25728–25733.

[Zheng et al., 1995] Zheng, Y., Bender, A., and Cerione, R. A. (1995). Interactions among proteins involved in bud-site selection and bud-site assembly in Saccharomyces cerevisiae. *Journal of Biological Chemistry*, 270(2):626–630.

[Zheng et al., 1994] Zheng, Y., Cerione, R., and Bender, A. (1994). Control of the yeast bud-site assembly GTPase Cdc42. Catalysis of guanine nucleotide exchange by Cdc24 and stimulation of GTPase activity by Bem3. *J Biol Chem*, 269(4):2369–2372.

[Zheng et al., 1993] Zheng, Y., Harts, M. J., Shinjosq, K., Evansn, T., Benderll, A., and Ceriones, R. a. (1993). Biochemical Comparisons of the Saccharomyces cerevisiae Bem2 and Bem3 Proteins. *Journal of Biological Chemistry*, 268(33):24629–24634.

Supplement S1

We developed a Cdc42 GTPase activity model for determining the GTPase cycling rates k. It is described in the following:

GTPase model

Cdc42 GTPase cycling involves three steps: (1) A GTP molecule from solution binds to Cdc42. (2) Cdc42 hydrolyses GTP. (3) Cdc42 releases GDP.

$$[\mathrm{GTP}] + [\mathrm{Cdc42}] \rightleftharpoons [\mathrm{Cdc42{-}GTP}]$$

$$[\mathrm{Cdc42{-}GTP}] \longrightarrow [\mathrm{Cdc42{-}GDP}]$$

$$[\mathrm{Cdc42{-}GDP}] \rightleftharpoons [\mathrm{Cdc42}] + [\mathrm{GDP}]$$

It can further be upregulated by effector proteins: GAPs have been shown to enhance GTP hydrolysis by Cdc42 (step 2), GEFs enhance the release of GDP from Cdc42 (step 3) [Park and Bi, 2007, Martin, 2015, Chiou et al., 2017].
To quantitatively describe the GTPase reaction cycle, we coarse-grained the GTPase reaction steps with

$$[\mathrm{GTP}] + n\,[\mathrm{Cdc42}] \longrightarrow [\mathrm{GDP}] + n\,[\mathrm{Cdc42}]$$

To account for possible Cdc42 dimerisation and cooperativity, we included the following reactions into the model:
(1) We assume that Cdc42 can dimerise, as other small GTPases have been shown to dimerise [Zhang and Zheng, 1998, Zhang et al., 1999, Zhang et al., 2001, Kang et al., 2010]:

$$2\,[\mathrm{mCdc42}] \rightleftharpoons [\mathrm{dCdc42}]$$

and both monomeric and dimeric Cdc42 can contribute to the overall GTP hydrolysis with different rates:

$$[\mathrm{GTP}] + [\mathrm{mCdc42}] \xrightarrow{k_1'} [\mathrm{GDP}] + [\mathrm{mCdc42}]$$

$$[\mathrm{GTP}] + [\mathrm{dCdc42}] \xrightarrow{k_2'} [\mathrm{GDP}] + [\mathrm{dCdc42}]$$

Assuming that the majority of Cdc42 is in its monomeric form ($[\mathrm{mCdc42}] < C_d$, with C_d as the concentration at which half of the total Cdc42 is dimeric), we can approximate

$$\begin{aligned} [\mathrm{dCdc42}] &= \frac{[\mathrm{mCdc42}]^2}{2C_d} \\ [\mathrm{mCdc42}] &\approx [\mathrm{Cdc42}] - \frac{[\mathrm{Cdc42}]^2}{C_d} \end{aligned} \tag{8}$$

(2) Next to cooperativity from dimerisation, cooperativity can also emerge when Cdc42 proteins come in close contact with each other - they can affect each other's behaviour without forming a stable homodimer, effectively functioning as an effector protein for themselves:

$$[\mathrm{GTP}] + 2\,[\mathrm{mCdc42}] \xrightarrow{k_3'} [\mathrm{GDP}] + 2\,[\mathrm{mCdc42}]$$

$$[\mathrm{GTP}] + [\mathrm{mCdc42}] + [\mathrm{dCdc42}] \xrightarrow{k_4'} [\mathrm{GDP}] + [\mathrm{mCdc42}] + [\mathrm{dCdc42}]$$

(3) Effector proteins, such as GAPs and GEFs, affect the speed of the GTP hydrolysis cycle:

$$[\mathrm{GTP}] + [\mathrm{Cdc42}][\mathrm{X}] \xrightarrow{k_5'} [\mathrm{GDP}] + [\mathrm{Cdc42}][\mathrm{X}]$$

Here X is an effector protein.

Our data showed that the amount of remaining GTP follows an exponential decline over time:

$$[\mathrm{GTP}]_t = [\mathrm{GTP}]_{t_0} \exp(-Kt)\text{, using } [\mathrm{GTP}]_{t_0} = 1 \tag{9}$$

Considering reactions (1) - (3), we can thus define K in Eq. 9 as

$$K = k_1'[\text{mCdc42}] + k_2'[\text{dCdc42}] + k_3'[\text{mCdc42}]^2 + k_4'[\text{mCdc42}][\text{dCdc42}] + k_5'[\text{Cdc42}][\text{X}]$$

Using Eq. 8, and considering only up to second-order terms, results in

$$\begin{aligned} K &= k_1'[\text{Cdc42}] + \left(\frac{k_2'}{2C_d} + k_3' - \frac{k_1'}{C_d}\right)[\text{Cdc42}]^2 + k_5'[\text{Cdc42}][X] \\ &= k_1[\text{Cdc42}] + k_2[\text{Cdc42}]^2 + k_{3,X}[\text{Cdc42}][\text{X}] \end{aligned} \tag{10}$$

where k_1 refers to GTP hydrolysis cycling rates of monomeric Cdc42, k_2 includes effects of cooperativity and dimerisation and k_3 represents the rate of Cdc42 - effector interaction. We refer to K as 'overall GTP hydrolysis rate'.

Variability between assays

We used Eq. 10 with [X]=0 to determine the rates of Cdc42 alone. We then conducted assays with Cdc42 and an effector protein to determine k_3. While doing so we needed to account for assay variability, i.e. for the observation that the rates for Cdc42 can vary between assays. Possible reasons for this include small concentration differences introduced though pipetting of small volumes (as are required for this assay), temperature and shaker speed fluctuations during the incubation step, and/or intrinsic changes in the protein activities due to other external conditions. To account for this variance, we introduced the parameter c_{corr}. It maps all factors that lead to variations between assays onto the Cdc42 concentration.
The assay data, including samples containing only Cdc42 and Cdc42 - (effector) protein mixtures, was fitted with

$$K = k_1 c_{corr}[\text{Cdc42}] + k_2(c_{corr}([\text{Cdc42}])^2 + k_{3,X}\, c_{corr}[\text{Cdc42}][\text{X}]$$

to determine c_{corr} and $k_{3,X}$ (using k_1 and k_2 determined earlier).
c_{corr} values spanned 0.5 to 1.3 (S5), with most values being close to 1.0, confirming that the variation between assays is small.

Cdc42 - effector interactions

In most cases, the the overall GTP hydrolysis rate depended linearly with increasing effector concentration X (Eq. 10). Exceptions were Cdc24 and Rga2.

Cdc24

Our data suggested that the GTP decline in assays Cdc42-Cdc24 mixtures does not depend linearly on the Cdc24 concentration (Fig. 3b), but is better approximated by a quadratic term:

$$K = k_1 c_{corr}[\text{Cdc42}] + k_2(c_{corr}([\text{Cdc42}])^2 + k_{3,Cdc24} c_{corr}[\text{Cdc42}][\text{Cdc24}]^2$$

We only included a quadratic Cdc24-term, as it fitted the data well an additional linear Cdc24-term ($k_{3,Cdc24,linear} c_{corr}[\text{Cdc42}][\text{Cdc24}]$) would have only introduced another fit parameter without contributing to the fit quality.

Rga2

In presence of up to 1µM Cdc42, the overall GTP hydrolysis rate increased linearly with Rga2 concentration up to 0.5µM Rga2. We used this regime for determining $k_{3,Rga2}$ and for assays in which both Rga2 and another protein was present (Eq. 2, 6).
We also developed a model to quantitatively fit data where higher Rga2 concentrations were used. This model describes the observed Rga2 behaviour (Fig. 3c green line). We did not use this model (and thus Rga2 concentrations outside of the linear regime) for further analysis, as this would make the obtained parameters less comparable (as they are based on different models and thus assumptions). The new model for Rga2 is described in the following:

In order to extend our coarse-grained model to accommodate GAP saturation, we must look in more detail to the steps that compose the GTP hydrolysis cycle. Concretely, consider the following reactions:

$$[GTP] + [Cdc42] \leftrightarrows [Cdc42 - GTP]$$

$$[Cdc42 - GTP] \longrightarrow [Cdc42 - GDP]$$

$$[Cdc42 - GDP] \leftrightarrows [Cdc42] + [GDP]$$

These leads to the following rate equations:

$$\frac{d[GTP]}{dt} = -k_b[Cdc42][GTP] + k_r[Cdc42 - GTP]$$

$$\frac{d[Cdc42]}{dt} = -k_b[Cdc42]([GTP] + [GDP]) + k_r[Cdc42 - GNP]$$

$$\frac{d[Cdc42 - GNP]}{dt} = k_b[Cdc42]([GTP] + [GDP]) - k_r[Cdc42 - GNP]$$

with GNP being either GTP or GDP. Without preferential attachment or dissociation for GTP and GDP, the number of bound nucleotides reaches an equilibrium. Thus, the time derivatives in the latter two rate equations equate to zero:

$$[Cdc42] = \frac{k_r}{k_b N_{tot}}[Cdc42 - GNP]$$

with N_{tot}=[GTP]+[GDP]. We can use the total concentration of Cdc42 (bound/unbound) molecules C_{tot} to yield for [Cdc42]:

$$C_{tot} = [Cdc42] + [Cdc42 - GNP] = \left(1 + \frac{k_b N_{tot}}{k_r}\right)[Cdc42]$$

$$\Longrightarrow [Cdc42] = \frac{C_{tot}}{1 + \frac{k_b N_{tot}}{k_r}}$$

Plugging this expression for [Cdc42] into rate equations for [GTP] and [Cdc42-GTP], we get:

$$\frac{d[GTP]}{dt} = -\frac{k_b C_{tot}}{1 + \frac{k_b N_{tot}}{k_r}}[GTP] + k_r[Cdc42 - GTP]$$

$$\frac{d[Cdc42 - GTP]}{dt} = k_b[Cdc42][GTP] - k_r[Cdc42 - GTP] - k_h[Cdc42 - GTP]$$

$$= \frac{k_b C_{tot}}{1 + \frac{k_b N_{tot}}{k_r}}[GTP] - (k_r + k_h)[Cdc42 - GTP]$$

In matrix form, these read as:

$$\frac{d}{dt}\begin{bmatrix} GTP \\ Cdc42 - GTP \end{bmatrix} = \begin{bmatrix} \frac{-k_b C_{tot}}{1 + \frac{k_b N_{tot}}{k_r}} & k_r \\ \frac{k_b C_{tot}}{1 + \frac{k_b N_{tot}}{k_r}} & -k_r - k_h \end{bmatrix}\begin{bmatrix} GTP \\ Cdc42 - GTP \end{bmatrix}$$

which is solved using the matrix exponential, using the initial condition that all GTP is free, scaling 100% as 1:

$$\begin{bmatrix} GTP \\ Cdc42-GTP \end{bmatrix} = \begin{bmatrix} 1 \\ 0 \end{bmatrix} e^{\begin{bmatrix} \frac{-k_b C_{tot}}{1+\frac{k_b N_{tot}}{k_r}} & k_r \\ \frac{k_b C_{tot}}{1+\frac{k_b N_{tot}}{k_r}} & -k_r - k_h \end{bmatrix} t}$$

The exponential decay with time of GTP (bound, unbound or total) equilibrates at a rate equal to minus the largest eigenvalue of the matrix in the exponential, thus:

$$rate = \frac{\left(\frac{k_b C_{tot}}{1+\frac{k_b N_{tot}}{k_r}} + k_r + k_h\right)}{2} - \frac{\sqrt{\left(\frac{k_b C_{tot}}{1+\frac{k_b N_{tot}}{k_r}} + k_r + k_h\right)^2 - 4\frac{k_b C_{tot}}{1+\frac{k_b N_{tot}}{k_r}} k_h}}{2}$$

Assuming the binding of nucleotide is relatively fast compared to its release, so if $k_b N_{tot} \gg k_r$, then:

$$rate = \frac{\left(\frac{k_r C_{tot}}{N_{tot}} + k_r + k_h\right)}{2} - \frac{\sqrt{\left(\frac{k_r C_{tot}}{N_{tot}} + k_r + k_h\right)^2 - 4\frac{k_r C_{tot}}{N_{tot}} k_h}}{2}$$

$$= \frac{\left(\frac{k_r C_{tot}}{N_{tot}} + k_r + k_h\right)}{2} - \frac{\left(\frac{k_r C_{tot}}{N_{tot}} + k_r + k_h\right)}{2}\sqrt{1 - 4\frac{k_r k_h C_{tot}}{N_{tot}\left(\frac{k_r C_{tot}}{N_{tot}} + k_r + k_h\right)^2}}$$

WE then assume there are much more nucleotides than Cdc42 molecules, so $C_{tot}/N_{tot} << 1$:

$$rate = \frac{k_r + k_h}{2} - \frac{\sqrt{(k_r + k_h)^2 - 4\frac{k_r C_{tot}}{N_{tot}} k_h}}{2} = \frac{k_r + k_h}{2} - \frac{k_r + k_h}{2}\sqrt{1 - 4\frac{k_r k_h C_{tot}}{N_{tot}(k_r + k_h)^2}}$$

and make the following approximation

$$4\frac{k_r k_h C_{tot}}{N_{tot}(k_r + k_h)^2} \ll 1 \Longrightarrow 2\sqrt{\frac{k_r k_h C_{tot}}{N_{tot}}} \ll k_r + k_h$$

which works best when the release and hydrolysis rates are not comparable. As we will be interested in the regime where we switch from hydrolysis rate-limited to release-rate limited, we will definitely be cutting corners here, but for the benefit of having a tractable, interpretable expression which will be easier to fit we will continue:
If

$$4\frac{k_r k_h C_{tot}}{N_{tot}(k_r + k_h)^2} \ll 1 \Longrightarrow 2\sqrt{\frac{k_r k_h C_{tot}}{N_{tot}}} \ll k_r + k_h$$

then

$$k_h = (\alpha + \beta[Rga2])(\gamma + \delta C_{tot}) = \alpha\gamma + \alpha d C_{tot} + \beta\gamma[Rga2] + \beta\delta C_{tot}[Rga2]$$

$$\approx \alpha\gamma + \alpha\delta C_{tot} + \beta\gamma[Rga2]$$

When hydrolysis is slow (compared to nucleotide release), the total rate increases linearly with increasing hydrolysis rate (as we used to model). At some point, hydrolysis then becomes sufficiently fast that release is rate-limiting, such that the total rate reaches a maximum of $k_r C_{tot}/N_{tot}$.

Now we can incorporate the GAPs, like Rga2, explicitly. We assume the hydrolysis rate is linearly dependent on GAP concentration and an additional linear dependency on [Cdc42] as described before.

$$rate = \frac{k_r k_h}{k_r + k_h}\frac{C_{tot}}{N_{tot}} = \frac{1}{N_{tot}}\frac{k_r C_{tot}(\alpha\gamma + \alpha\delta C_{tot} + \beta\gamma[Rga2])}{k_r + \alpha\gamma + \alpha\delta C_{tot} + \beta\gamma[Rga2]}$$

neglecting the higher-order term:

$$rate = \frac{k_r C_{tot}(\alpha\gamma + \alpha\delta C_{tot} + \beta\gamma[Rga2])}{k_r N_{tot}} = \frac{\alpha\gamma}{N_{tot}}C_{tot} + \frac{\alpha\delta}{N_{tot}}C_{tot}^2 + \frac{\beta\gamma}{N_{tot}}C_{tot}[Rga2]$$
$$= k_1 C_{tot} + k_2 C_{tot}^2 + k_3 C_{tot}[Rga2]$$

which is the functional form we used to have in the GTPase model, which assumed no such GAP saturation effects. More generally:

$$rate = \frac{k_r N_{tot}(k_1 C_{tot} + k_2 C_{tot}^2 + k_3 C_{tot}[Rga2])}{k_r N_{tot} + k_1 C_{tot} + k_2 C_{tot}^2 + k_3 C_{tot}[Rga2]}$$
$$= \frac{k_r'(k_1 C_{tot} + k_2 C_{tot}^2 + k_3 C_{tot}[Rga2])}{k_r' + k_1 C_{tot} + k_2 C_{tot}^2 + k_3 C_{tot}[Rga2]}$$

where we define $k_r \equiv k_r N_{tot}$ as the scaled nucleotide release rate. In assays where Cdc42 concentration is kept constant, the fit function would reduce to:

$$rate = \frac{c(a + b[Rga2])}{c + a + b[Rga2]}$$

where we estimate a, b and c. The parameters a and b would have the conventional interpretation in terms of k_1, k_2 and k_3. The parameter c is new and would be $k_r N_{tot}$.

Supplement S2

The pooled estimates of rates k_1, k_2, and k_3 were determined through weighting their standard error, as described in the following:

Within an assay, the rate parameters per run are calculated, but also a weighted average can be taken from these values to create a pooled estimate. Concretely:

For pooling, we model the n parameter estimates y_i to originate from a single pooled estimate a as:

$$\begin{bmatrix} y_1 \\ y_2 \\ \vdots \\ y_n \end{bmatrix} = a \begin{bmatrix} 1 \\ 1 \\ \vdots \\ 1 \end{bmatrix} + \begin{bmatrix} \varepsilon_1 \\ \varepsilon_2 \\ \vdots \\ \varepsilon_n \end{bmatrix}$$

with $\epsilon_i \sim N(0, \sigma_i)$ where σ_i is the standard error of the parameter estimate y_i. As uncertain estimates should be weighted less, the natural weights w_i to each y_i should be $1/\sigma_i$, after which all weighted errors follow a standard normal distribution:

$$\begin{bmatrix} w_1 y_1 \\ w_2 y_2 \\ \vdots \\ w_n y_n \end{bmatrix} = a \begin{bmatrix} w_1 \\ w_2 \\ \vdots \\ w_n \end{bmatrix} + \begin{bmatrix} w_1 \varepsilon_1 \\ w_2 \varepsilon_2 \\ \vdots \\ w_n \varepsilon_n \end{bmatrix} \Longrightarrow \begin{bmatrix} y_1^* \\ y_2^* \\ \vdots \\ y_n^* \end{bmatrix} = a \begin{bmatrix} w_1 \\ w_2 \\ \vdots \\ w_n \end{bmatrix} + \begin{bmatrix} \varepsilon_1^* \\ \varepsilon_2^* \\ \vdots \\ \varepsilon_n^* \end{bmatrix} \Longrightarrow \vec{y}^* = a\vec{w} + \vec{\varepsilon}^*$$

Getting the estimate for a, namely $\hat{a}$, is the result of a simple regression (i.e. weighted least squares), minimising the sum of squared errors (see e.g. [Heij et al., 2004]):

$$\hat{a} = \frac{\sum_{i=1}^{n} w_i y_i^*}{\sum_{i=1}^{n} w_i^2} = \frac{\sum_{i=1}^{n} w_i^2 y_i}{\sum_{i=1}^{n} w_i^2} = \frac{\sum_{i=1}^{n} \frac{y_i}{\sigma_i^2}}{\sum_{i=1}^{n} \frac{1}{\sigma_i^2}}$$

$$\sigma_{\hat{a}} = \frac{\frac{1}{n-1} \sum_{i=1}^{n} (w_i y_i - w_i \hat{a})^2}{\left(\sum_{i=1}^{n} w_i^2 \right)^2}$$

Supplement S3

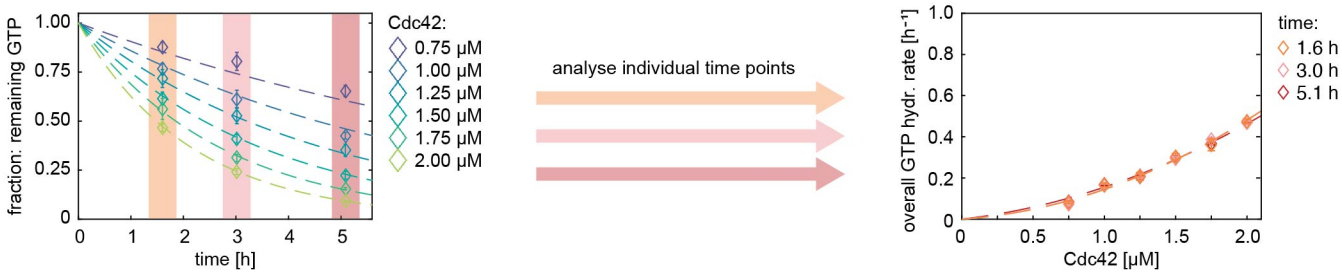

S3 Figure 1. The GTP concentration declines exponentially with time in GTPase reactions. Amount of remaining GTP for six Cdc42 concentrations and three time points (measured as one individual assay per time point). The remaining GTP content declines exponentially with time (left). Data of each individual time point shows the same overall GTP hydrolysis cycling rate for the Cdc42 concentrations. Thus, only one time point per assay condition is needed, to fit the data (right).

Supplement S4

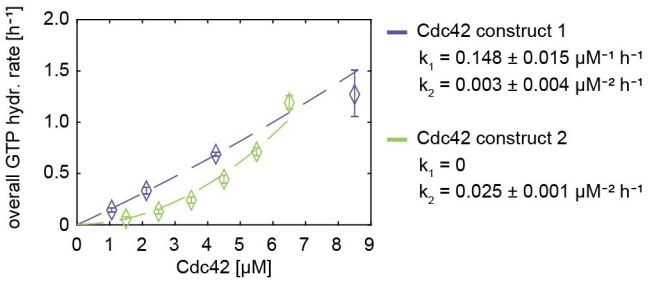

S4 Figure 1. Different Cdc42 constructs show varying degrees in cooperativity. The rate of Cdc42 construct 1 increases almost linearly with Cdc42 concentration (k_2[Cdc42]$^2 \ll k_1$[Cdc42] (in presence of 1 µM Cdc42)), and construct 2 can be described by only the quadratic term (k_1 = 0). A more detailed discussion is given in [Tschirpke et al., 2023].

Supplement S5

Data obtained from these GTPase assays is generally very reproducible [Tschirpke et al., 2023]. However, due to concentration differences introduced though pipetting of small volumes (as are required for this assay), temperature and shaker speed fluctuations during the incubation step, and/or intrinsic changes in the protein activities due to other external conditions, some variations in Cdc42 activity can occur. To account for this variance, we introduced the parameter c_{corr} to map all factors that lead to variations between assays onto the Cdc42 concentration:

$$[\text{GTP}]_t = [\text{GTP}]_{0h} \exp(-Kt)$$

$$\text{using } [\text{GTP}]_{0h} = 1 \text{ and } K = k_1 c_{corr}[\text{Cdc42}] + k_2 (c_{corr}[\text{Cdc42}])^2 + k_{3,X} c_{corr}[\text{Cdc42}][X]$$

c_{corr} values spanned 0.5 to 1.3, with most values being close to 1.0, confirming that the variation between assays is small (S5 Fig. 1).

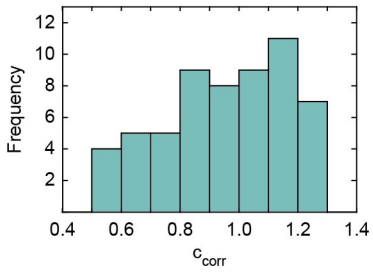

S5 Figure 1. The variation between GTPase assays is small. c_{corr} values are close to 1.

Supplement S6

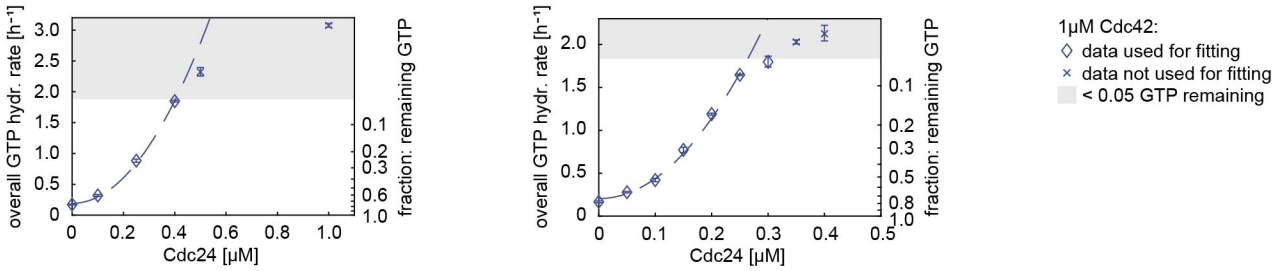

S6 Figure 1. Data points of less than 5% remaining GTP ought to be excluded. The effect of Cdc24 on the overall Cdc42 GTP hydrolysis rate seems to saturate for data points of less than 5% remaining GTP. The saturation effect correlates with being in a regime of little remaining GTP and does not reflect properties of Cdc24: it can be observed at 0.4 μM Cdc24 in one assay (left) and at 0.25 μM in another assay (right).

Supplement S7

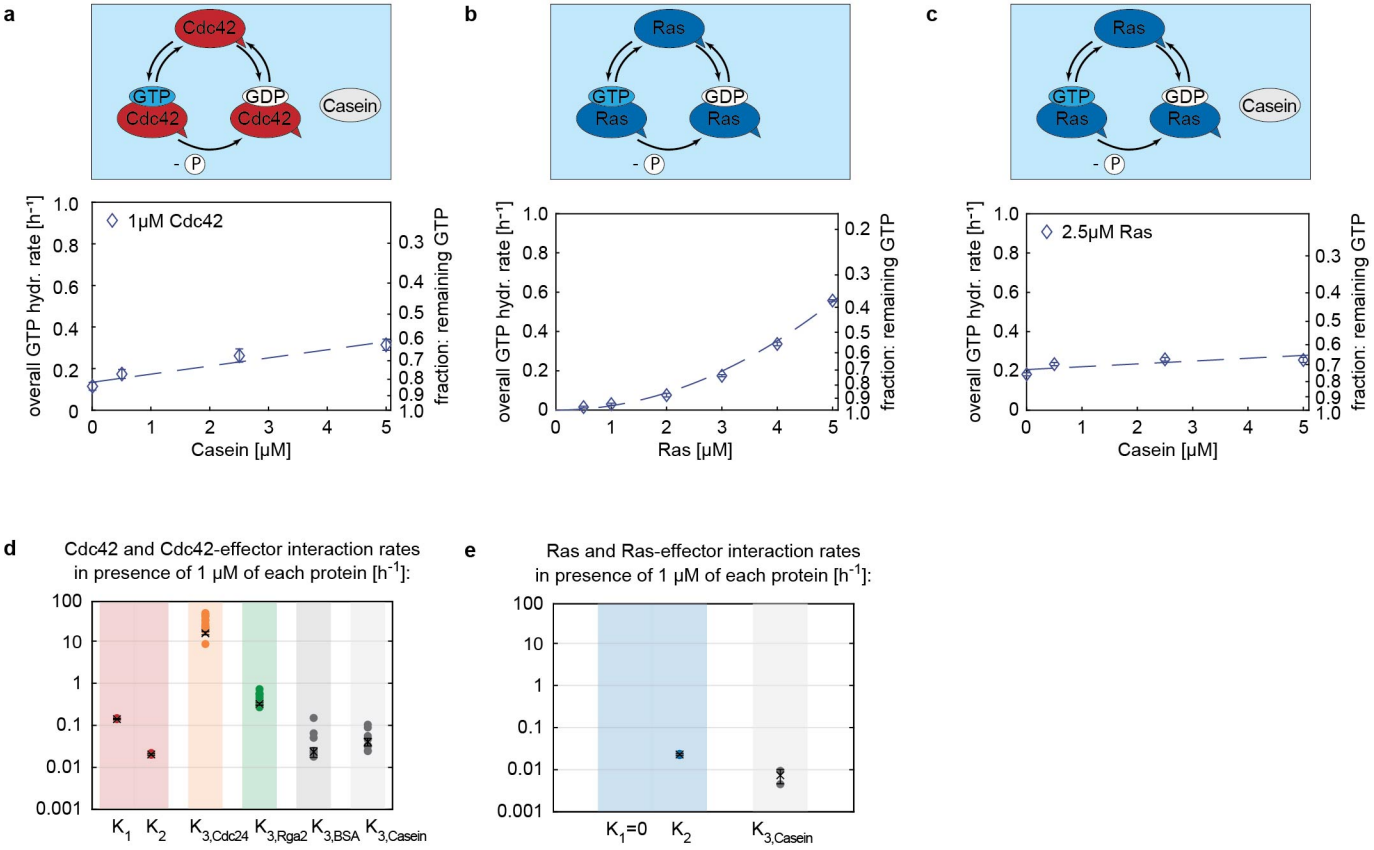

S7 Figure 1. Casein has a similar effect on Cdc42 as BSA. It also boosts GTP hydrolysis cycling of Ras, but to a smaller degree. (a) Casein increases the overall GTP hydrolysis rate of Cdc42 in a linear fashion. (b) The overall GTP hydrolysis rate of Ras increases quadratically with its concentration. (c) Casein increases the overall GTP hydrolysis rate of Ras in a linear fashion. (d,e) Overview of Cdc42-interactor (d) and Ras-interactor (e) rates. The values shown refer to the rate values in presence of 1µM of each protein, e.g. '$K_{3,Cdc24}$' refers to '$k_{3,Cdc24}$ [Cdc24]^2 [Cdc42]' with [Cdc42]=[Cdc24]=1 µM. (d) The rate of Casein ($k_{3,Casein}$) is comparable to that of BSA ($k_{3,BSA}$) but smaller than that of known Cdc42 effectors (Cdc24, Rga2). (e) Casein also effects Ras, but to a smaller degree than it does Cdc42. (a-e) An overview of all rate values is given in S9.

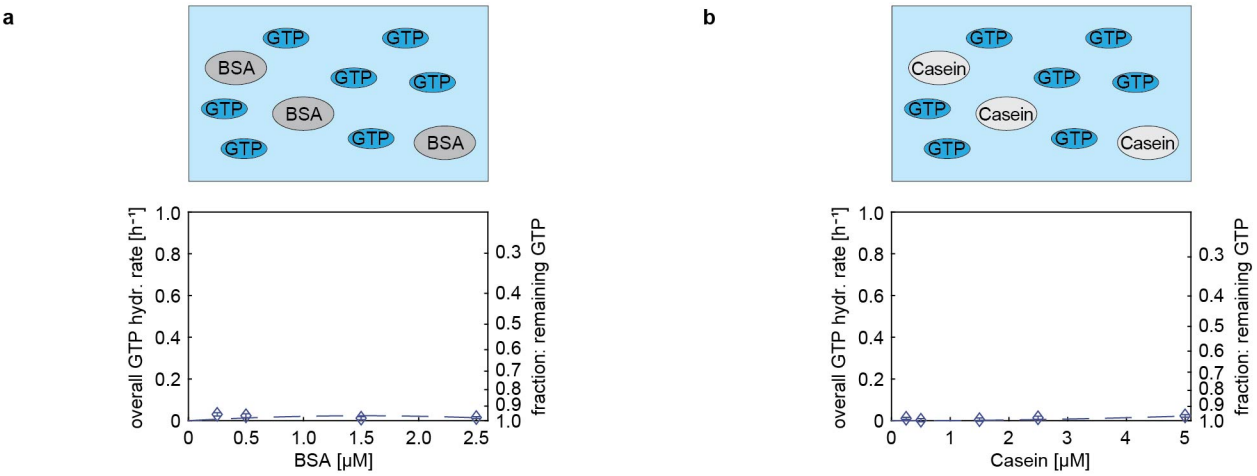

S7 Figure 2. In absence of any GTPase enzyme, BSA and Casein do not lead to GTP hydrolysis (or affect any downstream processing steps of the assay). (a) BSA inclubated with GTP. (b) Casein inclubated with GTP.

We observed an increase in the overall GTP hydrolysis rate of both Cdc42 and Ras in presence of BSA or Casein (Fig. 3 and S7 Fig. 1). In absence of a GTPase, neither BSA nor Casein lead to hydrolysed GTP (S7 Fig. 2), verifying that they do not cause GTP hydrolysis themselves and that they do not affect any downstream processes of the assay.

The effect of BSA/Casein on each GTPase enzyme (Cdc42, Ras) is about the same/an order of magnitude smaller than the GTPase rate values (Fig. 3d, S7 Fig. 1, S9), indicating that it mimics the effect of the GTPase it is incubated with. If some GTPase enzyme sticks to the reaction chamber wall and gets inactive (or less active) during the GTPase reacting, additions of any other BSA/Casein could increase the effective (active) GTPase concentration in the assay through sticking to the reaction chamber walls (thus leaving less spots where GTPases could stick). This would result in a perceived increase in the overall GTP hydrolysis rate.

However, Rho- and Ras-type GTPases (such as Cdc42 and Ras) have share conserved GTPase features [Bos et al., 2009] and the exact chemical reaction pathway of how these GTPases hydrolyse GTP is still debated [Calixto et al., 2020]. This allows for the possibility that BSA/Casein could also act as a GEF- or GAP-like protein towards both Cdc42 and Ras.

Further experiments are required to clarify this issue. For example, experiments focussing only on the GTP hydrolysis or GDP release step will show if BSA/Casein only affect one of these steps. A step-specific effect suggests that they interact with the GTPase and have a GEF- or GAP-like function. GTPase experiments, as conducted here, using GTPases that are more active than *S. cerevisae* Cdc42 or *H. sapiens* Ras (e.g. [Zhang et al., 1999, Caviston et al., 2002]). If the rate terms of BSA/Casein ($K_{3,BSA}/K_{3,Casein}$) correlate with K_1, K_2 of the GTPases, it suggests that the observed effect is due to BSA/Casein sticking to the reaction chamber walls, increasing the effective GTPase concentration.

Supplement S8

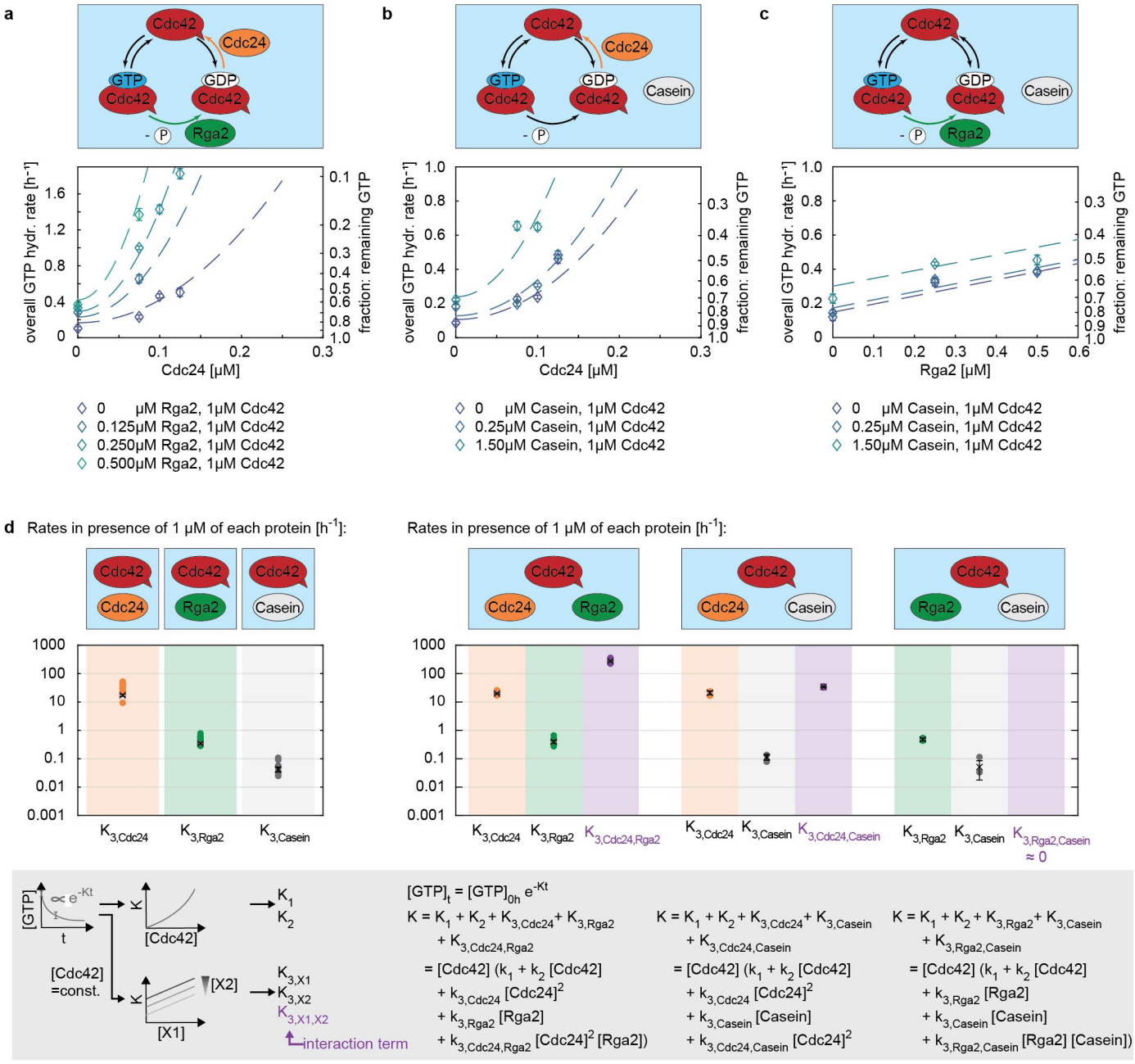

S8 Figure 1. Cdc24 and Rga2 synergistically boost GTPase cycling of Cdc42. Increase in the overall GTP hydrolsis cycling rate (K) of Cdc42 in presence of (a) Cdc24 and Rga2, (b) Cdc24 and Casein, and (c) Rga2 and Casein. (d) Illustration of the data processing and fitting model and summary of the obtained rates obtained in the three-protein assay (right) in comparison to those of the two-protein assay (left): In three-protein assays the rate contribution of the individual proteins is comparable to those obtained in the two-protein assay. Additionally, an interaction rate is obtained (shown in purple). This rate is huge in the case of Cdc42-Cdc24-Rga2 mixtures, indicating a strong synergy between Cdc24 and Rga2. In the case of Cdc42-Cdc24-Casein and Cdc42-Rga2-Casein mixtures, the interaction rate is comparable to the Cdc24 contribution/zero, indicating a weak/ almost no synergy. This effect could be due to non-specific protein-protein binding or because Casein coats to the reaction chamber wall, preventing the other proteins from binding, thus increasing the active concentration in the reaction. The values shown refer to the rate values in presence of 1μM of each protein, e.g. '$K_{3,Cdc24}$' refers to '$k_{3,Cdc24}$ [Cdc24]^2 [Cdc42]' with [Cdc42]=[Cdc24]=1 μM. Crosses with error bars represent the weighted mean and the standard error of the mean (S2), and filled circles show individual measurements. An overview of all rate values is given in S9.

Supplement S9

S9 Table 1. GTP hydrolysis cycling rates k_1 and k_2 of Cdc42 and Ras.

	k_1 [μM^{-1} h^{-1}]	k_1 std. err. [μM^{-1} h^{-1}]	k_2 [μM^{-2} h^{-1}]	k_2 std. err. [μM^{-2} h^{-1}]
pooled estimate Cdc42 (n=2)	0.148	0.004	0.021	0.001
pooled estimate Ras (n=2)	0	0	0.021	0.001

S9 Table 2. Interaction rates $k_{3,X}$ of Cdc42/Ras - effector protein mixtures. *: unit in case of X=Cdc24: [μM^{-3} h^{-1}].

	Effector protein X	$k_{3,X}$ [μM^{-2} h^{-1}] *	$k_{3,X}$ std. err.
Cdc42			
pooled est. (n=16)	Cdc24	17.239	1.524
pooled est. (n=14)	Rga2	0.345	0.024
pooled est. (n=6)	BSA	0.024	0.006
pooled est. (n=8)	Casein	0.042	0.009
Ras			
pooled est. (n=2)	Casein	0.007	0.002

S9 Table 3. Cdc42 - effector protein X interaction rates k_{3,X_1}, k_{3,X_2}, and k_{3,X_1,X_2}. *: unit in case of X_1=Cdc24: [μM^{-3} h^{-1}]. **: unit in case of X_2=Cdc24: [μM^{-4} h^{-1}].

	Effector protein X_1	Effector protein X_2	k_{3,X_1} [μM^{-2} h^{-1}] *	k_{3,X_1} std. err.	k_{3,X_2} [μM^{-2} h^{-1}]	k_{3,X_2} std. err.	k_{3,X_1,X_2} [μM^{-3} h^{-1}] **	k_{3,X_1,X_2} std. err.
pooled est. (n=6)	Cdc24	Rga2	19.898	1.143	0.395	0.051	275.343	19.940
pooled est. (n=2)	Cdc24	BSA	20.746	5.405	0.104	0.042	17.101	0.692
pooled est. (n=2)	Rga2	BSA	0.380	0.011	0.052	0.012	-0.073	0.008
pooled est. (n=2)	Cdc24	Casein	20.998	3.364	0.115	0.027	33.942	1.535
pooled est. (n=2)	Rga2	Casein	0.477	0.050	0.051	0.033	-0.050	0.016

Supplement S10

Cdc42, pRV007:

MGSSHHHHHHSSGLVPRGSHMASMTGGQQMGRGSEFDDDDKMQTLKCVVV GDGAVGKTCLLISYTTNQFPADYVPTVFDNYAVTVMIGDEPYTLGLFDTA
GQEDYDRLRPLSYPSTDVFLVCFSVISPPSFENVKEKWFPEVHHHCPGVP CLVVGTQIDLRDDKVIIEKLQRQRLRPITSEQGSRLARELKAVKYVECSA
LTQRGLKNVFDEAIVAALEPPVIKKSKKCAILLPETGGDYKDHDGDYKDH DIDYKDDDDK

Rga2, pRV014:

MGSSHHHHHHSSGLVPRGSHMASMTGGQQMGRGSEFDDDDKMSADPINDQ SSLCVRCNKSIASSQVYELESKKWHDQCFTCYKCDKKLNADSDFLVLDIG
TLICYDCSDKCTNCGDKIDDTAIILPSSNEAYCSNCFRCCRCSNRIKNLK YAKTKRGLCCMDCHEKLLRKKQLLLENQTKNSSKEDFPIKLPERSVKRPL
SPTRINGKSDVSTNNTAISKNLVSSNEDQQLTPQVLVSQERDESSLNDNN DNDNSKDREETSSHARTVSIDDILNSTLEHDSNSIEEQSLVDNEDYINKM
GEDVTYRLLKPQRANRDSIVVKDPRIPNSNSNANRFFSIYDKEETDKDDT DNKENEIIVNTPRNSTDKITSPLNSPMAVQMNEEVEPPHGLALTLSEATK
ENNKSSQGIQTSTSKSMNHVSPITRTDTVEMKTSTSSSTLRLSDNGSFSR PQTADNLLPHKKVAPSPNKKLSRSFSLKSKNFVHNLKSKTSEMLDPKHPH
HSTSIQESDTHSGWGVSSTHTNIRKSKAKKNPVSRGQSDSTIYNTLPQHG NFTVPEFNHKKAQSSLGSISKKQNSNDTATNRRINGSFTSSSSGHHIAMF
RTPPLESGPLFKRPSLSSESAHHRSSSLQTSRSTNALLEDDSTKVDATDE SATSLEKDFYFTELTLRKLKLDVRELEGTKKKLLQDVENLRLAKERLLND
VDNLTREKDKQSASSRESLEQKENIATSITVKSPSSNSDRKGSISNASPK PRFWKIFSSAKDHQVGDLESQQRSPNSSSGGTTNIAQKEISSPKLIRVHD
ELPSPGKVPLSPSPKRLDYTPDGSHLYGSSLQARCAYEKSTVPIIIRCCI DRIEKDDIGLNMEGLYRKSGSQTLVEEIENEFAQNNSLHSDTLSPKLNAL
LNQDIHAVASVLKRYLRKLPDPVLSFSIYDALIDLVRNNQLIERLPLNND KFLDSPQKVTIYEMVLKSLLEIFKILPVEHQEVLKVLAAHIGKVRRCSER
NLMNLHNLSLVFAPSLIHDFDGEKDIVDMKERNYIVEFILGNYRDIFKQA

Cdc24, pDM272:

MAIQTRFASGTSLSDLKPKPSATSISIPMQNVMNKPVTEQDSLFHICANI RKRLEVLPQLKPFLQLAYQSSEVLSERQSLLLSQKQHQELLKSNGANRDS
SDLAPTLRSSSISTATSLMSMEGISYTNSNPSATPNMEDTLLTFSMGILP ITMDCDPVTQLSQLFQQGAPLCILFNSVKPQFKLPVIASDDLKVCKKSIY
DFILGCKKHFAFNDEELFTISDVFANSTSQLVKVLEVVETLMNSSPTIFP SKSKTQQIMNAENQHRHQPQQSSKKHNEYVKIIKEFVATERKYVHDLEIL
DKYRQQLLDSNLITSEELYMLFPNLGDAIDFQRRFLISLEINALVEPSKQ RIGALFMHSKHFFKLYEPWSIGQNAAIEFLSSTLHKMRVDESQRFIINNK
LELQSFLYKPVQRLCRYPLLVKELLAESSDDNNTKELEAALDISKNIARS INENQRRTENHQVVKKLYGRVVNWKGYRISKFGELLYFDKVFISTTNSSS
EPEREFEVYLFEKIIILFSEVVTKKSASSLILKKKSSTSASISASNITDN NGSPHHSYHKRHSNSSSSNNIHLSSSSAAAIIHSSTNSSDNNSNNSSSSS
LFKLSANEPKLDLRGRIMIMNLNQIIPQNNRSLNITWESIKEQGNFLLKF KNEETRDNWSSCLQQLIHDLKNEQFKARHHSSTSTTSSTAKSSSMMSPTT
TMNTPNHHNSRQTHDSMASFSSSHMKRVSDVLPKRRTTSSSFESEIKSIS ENFKNSIPESSILFRISYNNNSNNTSSSEIFTLLVEKVWNFDDLIMAINS
KISNTHNNNISPITKIKYQDEDGDFVVLGSDEDWNVAKEMLAENNEKFLN IRLYLEHHHHHH

The protein constructs contain some of the following features:

- 6His-tag: HHHHHH
- Flag-tag: DYKDHDGDYKDHDIDYKDDDDK
- Thrombin cut site: LVPRGS
- Enterokinase cut site: DDDDK
- Sortase cut/ligation site: LPETGG
- T7 tag (to aid protein expression): MASMTGGQQMGRGSEF

More information on the protein constructs is given in [Tschirpke et al., 2023].

Supplement S11

S11 Table 1. Primer overview. List of primers used to generate plasmids of Tab 4. We used pET28a-His-mcm10-Sortase-Flag as the plasmid template (Tab 4). Abbreviations: ins: insertion; add: addition; fw: forward; rev: reverse.

Primer	Purpose	Sequence
oRV39	pRV007 gene fw	Gcaaatgggt cgcggatccg aattcGATGA CGACGATAAA ATGCAAACGC TAAAGTGTGT TGTTG
oRV40	pRV007 gene rev	CACCGTCGTG GTCCTTGTAG TCACCGCCGG TTTCCGGTAA CAAAATTGCA CATTTTTTAC TTTTCTTGAT AACAGG
oRV41	pRV007 vector fw	TTACCGGAAA CCGGCGGT
oRV42	pRV007 vector rev	TTTATCGTCG TCATCgaatt cggatcc
RV114	pRV014 gene fw	cgcggatccg aattcGATGA CGACGATAAA ATGTCAGCTG ACCCTATTAA TGACCAATCG TCTT-TATG
oRV115	pRV014 gene rev	GTTTCCGGTA AGCTTCCTCC GCCACCTTAT GCTTGCTTAA ATATGTCTCT ATAGTTTCCA A
oRV116	pRV014 vector fw	TTGGAAACTA TAGAGACATA TTTAAGCAAG CATAAGGTGG CGGAGGAAGC TTACCGGAAA C
oRV117	pRV014 vector rev	CATAAAGACG ATTGGTCATT AATAGGGTCA GCTGACATTT TATCGTCGTC ATCgaattcg gatc-cgcg